

Biology on a Chip: Microfabrication for Studying the Behavior of Cultured Cells

Nianzhen Li, Anna Tourovskaia, & Albert Folch

Department of Bioengineering, University of Washington, Seattle, Washington

Address all correspondence to Albert Folch, Campus Box 352255, University of Washington, Seattle, WA 98195, USA; afolch@u.washington.edu

ABSTRACT: The ability to culture cells *in vitro* has revolutionized hypothesis testing in basic cell and molecular biology research and has become a standard methodology in drug screening and toxicology assays. However, the traditional cell culture methodology—consisting essentially of the immersion of a large population of cells in a homogeneous fluid medium—has become increasingly limiting, both from a fundamental point of view (cells *in vivo* are surrounded by complex spatiotemporal microenvironments) and from a practical perspective (scaling up the number of fluid handling steps and cell manipulations for high-throughput studies *in vitro* is prohibitively expensive). Microfabrication technologies have enabled researchers to design, with micrometer control, the biochemical composition and topology of the substrate, the medium composition, as well as the type of neighboring cells surrounding the microenvironment of the cell. In addition, microtechnology is conceptually well suited for the development of fast, low-cost *in vitro* systems that allow for high-throughput culturing and analysis of cells under large numbers of conditions. Here we review a variety of applications of microfabrication in cell culture studies, with an emphasis on the biology of various cell types.

KEYWORDS: BioMEMS, cell culture microtechnology, microfluidics

I. INTRODUCTION

Despite constituting a simplistic simulation of the organism's inner workings, cell culture has become an essential tool in cell and molecular biology as well as in applied biotechnology. Cell culture systems inherently lack the three-dimensional, multicellular architecture found in an organism's tissue but offer precious advantages over whole-animal (*in vivo*) experimentation: (1) the parameters necessary for cell function can be isolated without interference from more complex, whole-organism or whole-organ responses; (2) because many experimental conditions can be tested with the cells from only one sacrificed animal, or a small portion of one, it reduces

animal care expenses, human labor costs, and animal suffering; (3) because the cells are distributed in a thin layer, optical observation under a microscope is unobstructed by other cell layers; and (4) with cell lines, the researcher effectively circumvents the time necessary to raise the animal and its very sacrifice; a wide range of sophisticated medium formulations and cell lines from almost any type of tissue are now commercially available.¹ However, cell culture technology is falling behind in the pace of progress: genes can now be probed simultaneously by the thousands on a DNA chip as animal genomes are being fully sequenced; biochemists can synthesize a combinatorial variety of drug candidates as well as myriad reporters that tag specific biomolecules and organic compounds that mimic the function of other biomolecules; and our molecular understanding of cell behavior is becoming a picture of pathways of biochemical reactions intricately entangled with each other. Yet cell culture methodology has remained basically unchanged for almost a century; it consists essentially of the immersion of a large population of cells in a homogeneous fluid medium. This requires at least one cell culture surface (such as a petri dish, a slide, or a well) for each cell culture condition to be investigated; in general, to account for statistical deviations and measurement errors, a few surfaces are used for each condition. Hence, as cells need to be fed periodically with fresh medium, the combinatorial testing of a variety of medium conditions involves large numbers of cell culture surfaces, bulky incubators, large fluid volumes, and expensive human labor and/or equipment (see Fig. 1).

Microfabrication technology, a generic term that encompasses any technique that allows for manufacturing miniature components and devices with micrometer (or submillimeter) resolution, has an inherent potential for the development of fast, inexpensive cell culture systems that produce results at high throughput—i.e., probing large numbers of single cells under large numbers of conditions. It is important to note that the introduction of microfabrication in cell culture technology is advantageous not only to increase experimentation throughput. In addition, cellular processes such as adhesion, migration, growth, secretion, and gene expression are triggered, controlled, or influenced by the biomolecular three-dimensional organization of neighboring surfaces. This organization cannot be straightforwardly reproduced in the laboratory. Indeed, cells respond to *local* concentrations of a variety of molecules that may be dissolved in the extracellular medium (e.g., enzymes, nutrients, small ions), present on the underlying surface (e.g., extracellular matrix proteins) or on the surface of adjacent cells (e.g., membrane receptors) (Fig. 2). In traditional cell culture, these factors are varied homogeneously across the substrate. Microfabrication techniques enable researchers to design, with micrometer control, the biochemical composition and topology of the substrate—otherwise homogeneously adherent to cells—the medium composition, as well as the type of cell surrounding each cell. Furthermore, recent work in three-dimensional (3-D) culture systems has exposed significant limitations of studying cells on flat (two-

BIOLOGY ON A CHIP

Large numbers of cells and supplies



Human labor



Animal suffering



Expensive equipment



FIGURE 1. Limitations of traditional cell culture methodology. Conventional cell culture techniques usually consist of the immersion of a large population of cells in a homogeneous fluid medium, resulting in use of large numbers of cell and supplies, animal suffering, expensive equipments, and intensive human labor.

dimensional, 2-D) surfaces. Techniques for microfabricating 3-D scaffolds may be applicable to 3-D cultures.²⁻⁵

In this review, we introduce the reader to various applications of microfabrication techniques in cell biology, focusing on how one can (1) microengineer the extracellular substrate for cell adhesion (micropatterning), (2) microengineer the delivery of soluble factors to cells (microfluidic delivery), and (3) microengineer the measurement of cellular properties. An effort has been made to subdivide the review

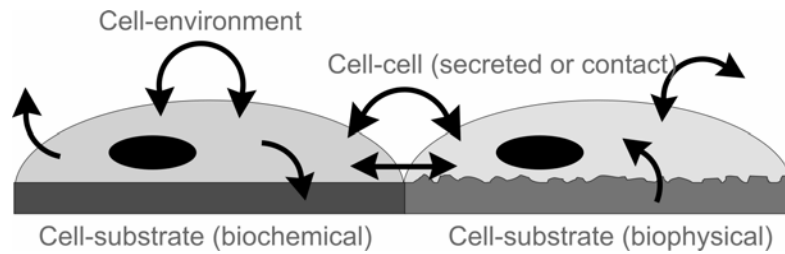


FIGURE 2. Local signals regulate cell behavior. Cellular processes such as adhesion, migration, growth, secretion, and gene expression are triggered, controlled, or influenced by *local* biophysical and biochemical signals, such as time-varying concentrations of a variety of molecules, which may be dissolved in the extracellular medium (e.g., enzymes, nutrients, small ions), present on the underlying surface (e.g., extracellular matrix proteins) or on the surface of adjacent cells (e.g., membrane receptors).

according to the biological questions that were addressed in each work rather than by the technical accomplishments. Because the questions most often are specific to a given cell type, the review's sections are categorized according to the cell type that was used in each study.

II. GENERAL MICROFABRICATION TECHNIQUES

A wide range of microfabrication techniques has been developed to produce miniature components and devices with micrometer-scale resolution. Although most of these techniques were initially developed for the semiconductor industry to fabricate integrated circuits, they have been adopted and modified to manufacture a large variety of tools and materials for biological research. The following is a brief overview of the most common microfabrication techniques used for biomedical applications, intended for the purpose of introducing terminology. For more detailed coverage on traditional microfabrication methods see, Refs. 6–9.

II.A. Photolithography

Photolithography is historically the most widely used micropatterning technique; with photolithography, the size of the features can be precisely controlled (de-

pending on the photomask resolution) down to micrometer dimensions—a size domain comparable or smaller than a single cell. It is essentially based on the selective exposure of a thin film of a light-sensitive organic polymer (photoresist) to light. Generally, photoresist solution is dispensed onto a flat substrate, usually a silicon or glass wafer, spun into a thin film, and dried (Fig. 3A). When this photosensitive layer is exposed to UV light through a “photomask”—a transparent plate with the desired opaque pattern on its surface (Fig. 3B)—the regions of the photoresist exposed to the light undergo a chemical modification. In the case of a “positive” photoresist (by definition), the irradiated polymer molecules break down and become much more soluble in a specific developer solution than the unexposed regions. In the case of a negative photoresist (e.g., the widely used “SU-8” photoresist developed by IBM to produce tall structures), light induces photochemical crosslinking of the photoresist, which renders the exposed regions virtually insoluble in the developer (Fig. 3C).

The resulting photoresist patterns can be used as lift-off masks for patterning of biomolecules—e.g., to create cell-repellent and/or cell-adhesive substrates. The material of interest is deposited on the photoresist pattern, and the photoresist is lifted off (often by sonication in acetone) leaving the desired biomolecule pattern. This approach has the drawbacks that exposure to organic solvent (if the photoresist is to be removed) leads to denaturation of most biomolecules, which may or may not be a concern, and makes it incompatible with many polymers widely used in cell culture (such as polystyrene, which dissolves in acetone). Although water-soluble photoresists exist, there is still a concern that photoresist residues may be left on the surface if the surface cannot be cleaned thoroughly after processing, because it is partially covered by biomolecules. The first example is found in the work of Kleinfeld et al.,¹⁰ who pioneered the use of micropatterns of self-assembled monolayers (SAMs) to micropattern cells; they created micropatterns of embryonic mouse spinal cells and perinatal rat cerebellar cells on alternating stripes of aminosilane and methyl-terminated alkylsilane SAM. The SAM patterns were created by photolithography, using photoresist as a mask for the chemisorption of silanes, which are unaffected by the photoresist dissolution process. Only the areas derivatized with diamines and triamines—but not monoamines—promoted the adhesion of embryonic mouse spinal cells and perinatal rat cerebellar cells, and morphology was assessed to be very similar to that of cultures on poly D-lysine (PDL). Patterns of the cerebellar cells were preserved for at least 12 days, which allowed for the development and observation of electrical excitability. The goal of using methyl-terminated alkylsilanes was to recreate the hydrophobicity of certain surfaces that inhibit cell adhesion; however, other researchers have created cellular micropatterns where cells attach precisely to methyl-terminated areas.

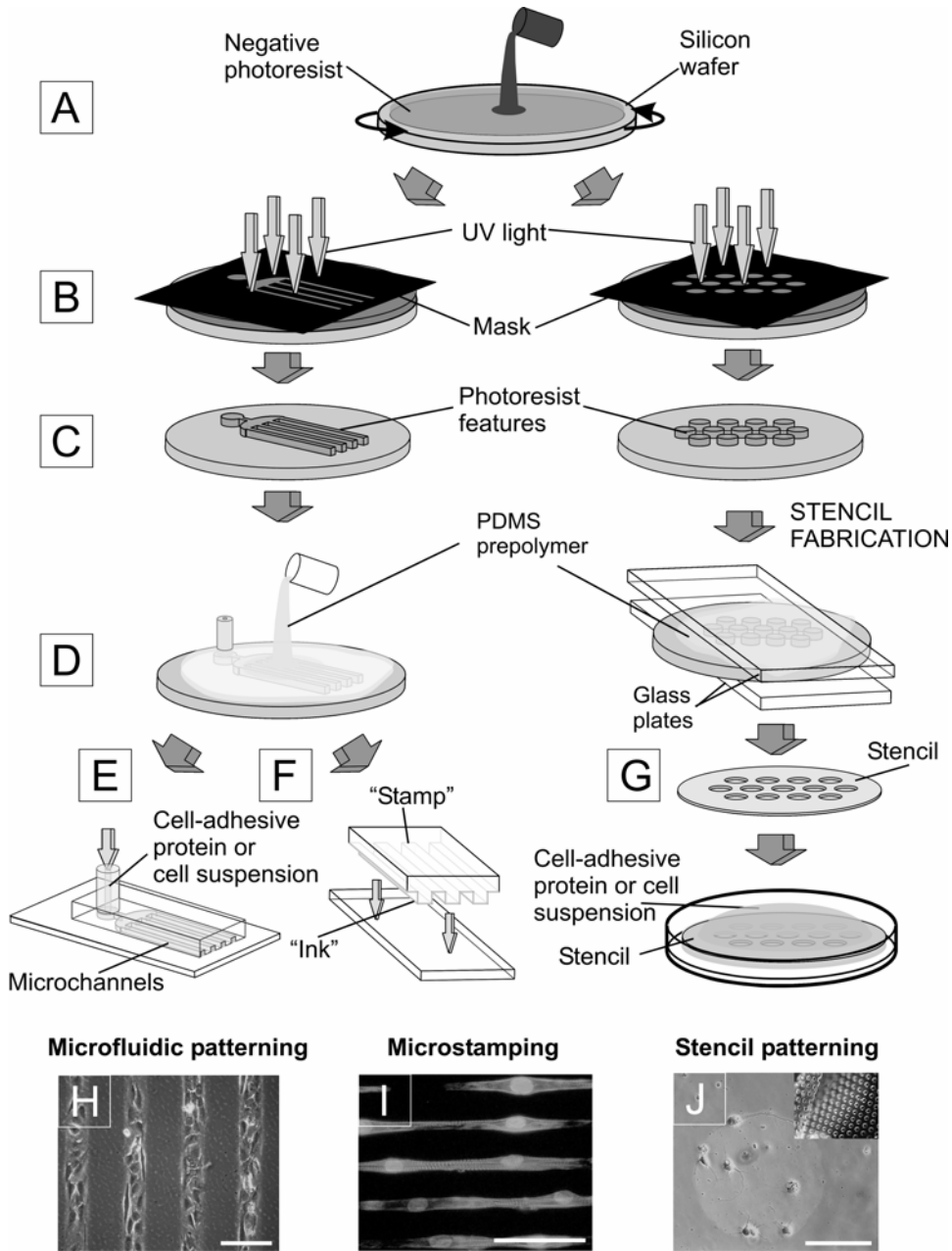


FIGURE 3. General process flow in soft lithography, which typically requires photolithography to create a mold or "master." **(A)** Photoresist solution is dispensed onto a silicon wafer, and spun into a thin film, with the height controlled by the viscosity of the solution and the spin speed. **(B)** When the photosensitive layer is exposed to UV light through a photomask with the desired opaque patterns, the regions of the photoresist exposed to the light undergo a chemical modification. **(C)** In the case of a "negative" photoresist such as SU-8, UV light induces

II.B. Micromachining (Etching and Deposition)

Micromachining refers to the creation of topographical features on a surface by means of etching or deposition.⁶⁻⁹ A photolithographically defined photoresist micropattern can be used as a protective “mask” (not to be confused with the “photomask” in photolithography) to transfer the pattern to an underlying layer. The etching can use liquid chemicals (wet etch) or ion plasmas (dry etch), and be isotropic (the etch proceeds in depth as well as sideways) or anisotropic (the etch proceeds in a preferred direction). Resists made of SAMs can also be used as masks for isotropic wet etchants on a limited set of substrates (mainly, metals or oxides).¹¹ Photoresist patterns can also be used to mask the deposition of metals (Au, Ag, etc.).

II.C. Soft Lithography

Soft lithography¹² refers to a set of sister techniques pioneered by Whitesides and colleagues that are all based on the replica molding of microstructures in poly(dimethylsiloxane) (PDMS), a transparent silicone rubber. Although soft lithography typically requires a photolithographic step (and thus access to a clean room) to fabricate the mold, the mold can be reused so routine access to a clean room is not essential. It is important to note that PDMS is very suited for biological applications,¹²⁻¹⁵ because it is biocompatible (cells can be cultured atop it), transparent (e.g., for phase-contrast microscopy), inexpensive (both the material and the straightforward molding process), permeable to gases (dead-end channels can be filled by pushing the fluid in), and amenable to surface modification (which can, in principle, be used to change the chemical or biological functionality of the PDMS surface). PDMS can replicate submicron features with high fidelity, can form a reversible seal with smooth surfaces (hence the PDMS microstructures surface can be used to form microfluidic circuits), and when oxidized by simple exposure to oxygen

crosslinking of the photoresist, rendering the exposed regions insoluble in the developer, which results in a pattern that is a negative image of the mask. **(D)** Liquid PDMS precursor is mixed with its curing agent and poured over the master’s pattern, then cured at a raised temperature; and finally the cured PDMS replica is peeled off from the master. Masters can be reused to make more replicas. **(E–G)** are example of PDMS devices used in surface micropatterning. **(E)** A microchannel device for microfluidically patterning surface proteins and cells, resulting in **(H)** patterns of fibronectin and fibroblasts (unpublished results from the Folch lab). **(F)** A microstamp absorbed with protein “ink” (fibronectin) for micropatterned spreading and differentiation of **(I)** cardiac myocytes (contributed by McDevitt et al.²²⁵). **(G)** A stencil with through-holes to micropattern **(J)** neurons on polylysine patterns (unpublished results from Folch lab; inset shows a picture of a PDMS stencil). Scale bars are 100 μm .

plasma, it can be irreversibly bonded to itself, glass, silicon, polystyrene, polyethylene, and silicon nitride, provided that these surfaces have also been exposed to air plasma. In many cases, the PDMS replica itself can be reused indefinitely.

Unlike photolithography, the success of a soft lithographic process is dependent on the actual pattern design and alignment of features in separate patterning steps is challenging (because of the flexibility of PDMS). Examples of three important soft lithographic processes are shown in Figure 3. Soft lithography starts with photolithography (Fig. 3A and B) to microfabricate the “master” (Fig. 3C), then the master is replicated in PDMS (Fig. 3D–G). The replication process consists simply of pouring a liquid PDMS precursor (a two-part mixture that contains a cross-linker and monomers) over the master (Fig. 3D). (Alternatively, PDMS molds can be used as masters provided they are surface treated to prevent them from bonding to the curing PDMS.) The PDMS precursor is cured at a raised temperature in order to accelerate the curing reaction. Finally, the cured PDMS is peeled off from the master, which generally withstands the replication process and can be reused.

1. Microfluidic Patterning

Figure 3E depicts a method we dub microfluidic patterning, whereby microchannels (formed by sealing a PDMS mold against a substrate) are used to route fluids to selected areas of the substrate; originally devised for patterning polymers by capillarity,¹⁶ the microfluidic patterning of proteins (also by capillarity) was pioneered by Biebuyck’s group¹⁷; unfortunately, capillarity-driven flow limits the technique to small areas and channels—clearly not suited for cellular studies. Toner’s group extended the concept to large-area patterning of proteins or gels¹⁸ and cells¹⁹ by using pressure-assisted flow. The molding of PDMS microchannels featuring large cross-sections¹⁹ was possible with the introduction of the SU-8 family of negative photoresist by IBM (capable of yielding tall structures with vertical walls using standard mask aligners). Microfluidic patterning is compatible with the traditional, simple protocols for protein and cell attachment widely used in cell culture, but it is restricted to interconnected patterns unless a 3-D microfluidic network is constructed.²⁰ It is important to note that laminar flow conditions typical of microchannels allows for patterning several fluids in parallel streams in one channel²¹ and for creating well-defined fluid gradients.²²

2. Microstamping

Figure 3F depicts *microcontact printing*, popularly known as *microstamping*, whereby the PDMS mold is used as a stamp to transfer “ink”; note that, as opposed to

microfluidic patterning, the transfer occurs where the stamp contacts the surface. Originally demonstrated for alkanethiol inks transferred on gold for producing patterns of SAMs,¹¹ the principle works also for the transfer of dried proteins from PDMS to various surfaces, as demonstrated by three groups simultaneously.²³⁻²⁵ Although microstamping of proteins represents a protein immobilization protocol (based on contact transfer of a dry layer) that departs substantially from the traditional one (based on deposition from solution), it is experimentally simple and allows for greater flexibility and resolution than microfluidic patterning. Alignment of two non-overlapping protein patterns is facilitated by the use of a single multilevel stamp.²⁶

3. Stencil Patterning

Figure 3G depicts *stencil patterning*, whereby a PDMS membrane is fabricated by exclusion of PDMS from the top of the photoresist master features, resulting in holes with the shape of the master features. PDMS can be excluded from the top of the features by (1) pressing a plate against the master after the PDMS has been poured over the master,²⁷ (2) capping the dry master with a cover (which effectively forms a microfluidic chamber) and using suction or injection to fill the space between the cover and the master,^{27,28} or (3) spinning a PDMS prepolymer on the master with photoresist posts to a thickness smaller than the height of the posts.^{29,30} The stencil can be used as a mask for selective adsorption of cell-adhesive proteins to promote selective cell attachment (Fig. 3G) or can be directly seeded on the stencil-covered substrate; after the stencil is peeled off, surface cellular “islands” with the same shape of the holes remain on the surface. Although the stencil can be difficult to handle (see an example of a stencil in Figure 3J inset), the technique is straightforward and can be combined with virtually all cell types and substrates, even curved or moist.²⁷ Compared to microfluidic patterning devices, high-resolution stencils are more difficult to fabricate and work best with regular pattern designs, but they allow for disconnected patterns down to the single-cell level^{27,30} and unlimited exposure of the cells to the device.

Figure 3H, I, and J show cellular micropatterns created by microfluidic patterning, microstamping, and stencil patterning, respectively; in all cases, the cellular micropatterns were created indirectly by first producing a substrate with differential cellular adhesiveness: the cells attached selectively to a cell-adhesive molecule (fibronectin lines in Fig. 3H and I, poly lysine circle in Fig. 3J) surrounded by a nonadhesive background (albumin adsorbed on polystyrene in Fig. 3H and I, plain glass in Fig. 3J), whereas the nonattached cells were washed away.

III. ENGINEERING SURFACE COMPOSITION

Cell adhesion is mediated in part by cell-membrane-bound receptors (in particular, integrins, a family of heterodimeric transmembrane proteins that are linked to the cytoskeleton on the cytoplasmic side of the membrane), which recognize specific peptide sequences present in the extracellular matrix (ECM) proteins.³¹ Integrins aggregate in organized structures termed *focal contacts*,³²⁻³⁴ which establish a mechanical link between the membrane and the ECM substrate and between the ECM and the cytoskeleton. In most cell types, certain biochemical signals essential for cell growth, function, and survival are triggered by integrins upon attachment; without attachment, the cell undergoes apoptosis.³⁵ Because many cell types secrete ECM and most surfaces readily support protein adsorption, an artificial substrate may support cell adhesion even if it is not initially coated with ECM and/or the cells are cultured in the presence of medium containing serum (which contains adhesive proteins).

III.A. Engineering Cell-Adhesiveness of a Substrate

Cellular micropatterning methods may attempt to engineer cell-adhesive surfaces of metals, polymers, proteins, etc. and/or cell-repellent surfaces (then, the cells attach to their preferred substrate), or may use a physical barrier such as a stencil^{27,30} or a microchannel^{19,20} that can be removed after cell attachment—ideally, without inflicting damage to the cells. Materials other than physiological biomolecules were the first to be explored for selective cell adhesiveness because of the constraints imposed by early micropatterning techniques.³⁶ The mechanisms for immobilizing biomolecules can consist of physisorption (i.e., physical immobilization or “adsorption” of proteins or polyamines) or chemisorption (i.e., covalent immobilization of synthetic peptides, polymers, etc.). Commonly used cell-repellent surface modifications for micropatterning³⁶ include physisorbed albumin,³⁷ micromolded agarose,¹⁸ and covalently linked polymers such as poly(ethylene glycol) (PEG).

We note that cell adhesiveness selectivity is highly dependent on the cell type, the duration of the exposure of the cells to the pattern, the cell density, and the composition of the medium. As an example, Toner’s group^{18,38,39} exploited this differential adhesiveness to create cocultures of two cell types—hepatocytes and fibroblasts—on micropatterns of collagen (cell adhesive) surrounded by albumin (nonadhesive); the pattern is “respected” by either cell type only if the cell culture medium is free of serum proteins—presumably, because serum contains adhesive proteins that adsorb onto albumin, rendering the albumin-coated areas adhesive. Hence, hepatocytes were seeded first in serum-free medium, resulting in hepatocytes adhered to the collagen areas, and later fibroblasts were seeded in serum-contain-

ing medium, resulting in attachment of fibroblasts on the initially albumin areas. The technique does not work well if the order of patterning is inverted, because hepatocytes form a very compact monolayer of polygonal cells at confluence, leaving virtually no area for the fibroblasts to attach; fibroblasts, on the other hand, have irregular shapes that do not necessarily optimize substrate coverage. Obviously, the technique is only successful for confluent monolayers of cells—i.e., it fails for sparse cultures, because it relies on 100% occupancy of the adhesive-protein areas after the first cell type seeding.

A widely used surface chemical modification is the close-packed SAM formed by some organic molecules.⁴⁰ Upon formation of a complete monolayer, the chemical nature of the surface is no longer defined by the composition of the underlying substrate but by the exposed functional groups of the monolayer. SAMs of different end functionalities have been used to tailor surface properties for adhesion,⁴¹ lubrication,⁴² wettability,⁴³ or protein physisorption.⁴⁴ Moreover, SAMs may be functionalized with reactive groups to which biological material is subsequently attached. Biomolecules may be immobilized either directly or by attaching an intermediate “tether” or crosslinker onto the monolayer.⁴⁵ SAMs, whose end functionalities are recognized by cell membrane receptors^{31,46,47} or by tagged proteins,^{48,49} are also possible. Although organic polymers have a poorly characterized surface composition, they are also amenable to SAM derivatization after certain chemical treatments.^{45,50-56} Despite issues of monolayer order and biointeraction, the use of SAMs in biopatterning is appealing because the adhesiveness of the surface is engineered at a molecular level,⁵⁷ and at the same time biopatterning is reduced to patterning the SAM.⁵⁸

III.B. Switchable Substrates

A particular class of surface engineering method is that of substrates of “switchable” cell adhesiveness. The first reported switch was thermally actuated, using the thermo-responsive polymer poly *N*-isopropyl acrylamide (PNIPAAm), which is hydrophobic above the lower critical solubility temperature (LCST, ~32 °C) and very hydrophilic below the LCST. Takezawa et al.⁵⁹ conjugated PNIPAAm to collagen as a substrate for culturing of human dermal fibroblasts and showed that cells could spread and grew normally on this surface above the LCST but could be detached by lowering the temperature below the LCST without the use of conventional (damaging) enzymes such as trypsin. Without compromised functions found in cultured cells damaged by trypsinization, cells recovered by this method maintained substrate adhesivity, growth, and secretion activities similar to those of primary cultured cells. It is important to note that the thermo-responsive polymer can be micropatterned on substrates by photolithography, so that cells can be selectively detached from the

polymer-grafted regions. Mouse fibroblasts grown on the copolymer-grafted surface area were selectively detached by lowering the temperature in serum-free medium, but only partially detached in serum-containing medium.^{60,61} Growth factors such as insulin could also be immobilized to the thermoresponsive polymer and showed stimulation of cell growth.^{62,63}

Mrksich et al.⁴⁷ developed an electrochemical switch to reverse the cell adhesiveness of a substrate (or select regions of a substrate). The method was based on a mixed SAM of alkanethiolates on gold that presents hydroquinone groups among a background of penta(ethyleneglycol) groups. When an electrical potential is applied to the underlying gold film, the hydroquinone group undergoes oxidation to give the corresponding benzoquinone, which then reacts with cyclopentadiene to afford a covalent adduct. Conjugates of cyclopentadiene and the peptide Gly Arg-Gly Asp-Ser-NH₂ (RGD-Cp) were immobilized to make the surface cell adhesive. SAMs were patterned into regions having this electroactive monolayer and a second set of regions that were cell adhesive (methyl-terminated SAMs). Similarly, Jiang et al.⁶⁴ prepared micropatterns of an oligo(ethyleneglycol)-terminated SAM (preventing cell adhesion) and a methyl-terminated SAM (allowing adsorption of proteins and attachment of bovine capillary endothelial cells); the oligo(ethyleneglycol)-terminated SAM can be desorbed by application of a voltage pulse, thus allowing proteins to adsorb onto previously inert areas and enabling cells to migrate into these areas.

III.C. Surface Gradients

Gradients of immobilized biomolecules are useful for investigating the response of cells to changes in concentration (i.e., haptotaxis studies), and to large numbers of biomolecule concentration values (i.e., high-throughput studies). If the biomolecule can be photochemically immobilized, the generation of a gradient is a matter of generating a graded light exposure. Chen and Ito⁶⁵ created a micropattern of photo-immobilized epidermal growth factor (EGF) using a photomask with a gradient pattern (transparent 2- μm -wide lines separated by gaps of 4–30 μm width of varying opacity). EGF was conjugated with photoreactive azidophenyl-derivatized polyallylamine. CHO cells overexpressing EGF receptor proteins exhibited enhanced growth on higher density (smaller gap) of immobilized EGF. Herbert et al.⁶⁶ photo-immobilized micropatterns of Arg-Gly Asp (RGD) sequence-containing oligopeptides on an oligo(ethylene glycol) alkanethiolate SAM. The pattern and amount of immobilized RGD were controlled by manipulating the duration of UV exposure through a photomask, resulting in a surface density gradient of immobilized peptides. In serum-free medium, the number of attached fibroblasts increased with increasing RGD concentration.

Microfluidic patterning methods can be used for biomolecules that cannot be photochemically immobilized. Whitesides and coworkers^{22,67} generated solution and

surface gradients using controlled diffusive mixing of species in laminar flow in PDMS microfluidic networks. Flowing multiple streams of fluid each carrying different concentrations of substances side by side generated step concentration gradients perpendicular to the direction of the flow. Complex shapes of gradient (linear, parabolic, and periodic) can be generated by proper design of the microchannels.²² The lateral dimensions of the gradients, determined by the width of the microchannels, ranged from 350 to 2200 μm . Using this method, complicated shapes of laminin gradients were created on poly L-lysine-coated PDMS substrates, and rat hippocampal neurons were cultured on these substrate-bound gradients. Axons showed preference orienting to the direction of increasing surface density of laminin. Linear gradients in laminin adsorbed from a gradient in solution having a slope of laminin concentration larger than $\sim 0.06 \mu\text{g}/(\text{mL} \times \mu\text{m})$ (defined by dividing the change of laminin concentration in solution over the distance of the gradient) oriented axon specification, whereas those with laminin concentration smaller than $\sim 0.06 \mu\text{g}/(\text{mL} \times \mu\text{m})$ had no effect.⁶⁸

IV. ENGINEERING FLUID ENVIRONMENTS

In traditional cell cultures, medium changing or the application of a drug or a biological soluble factor often involves the use of pipettes, either a “macro” serological pipette (sometimes a perfusion system consisting of input and suction pipettes) for large-volume application to cell populations, or a micropipette for localized application to single cells. Those procedures are labor intensive and unscalable, and their reliability is often low and highly user dependent. Given these limitations, microfluidic devices represent a technology with great promise for cell culture studies.

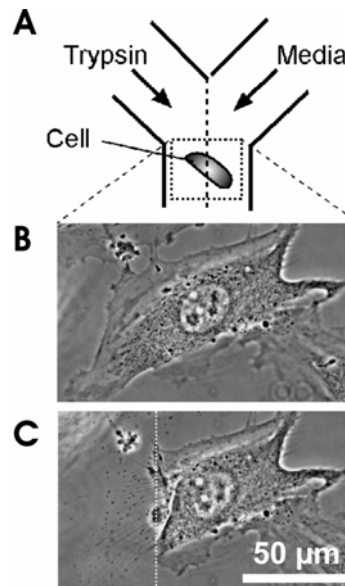
Microfluidics is the handling and analyzing of fluids in sub-millimeter-scale volumes. At the microscale, different forces become dominant over those experienced in everyday life. The physicochemical phenomena that become important in microfluidics include laminar flow, diffusion, fluidic resistance, surface-area-to-volume ratio, and surface tension.⁶⁹ In small (hundreds of microns) channels with slow flow, the Reynolds number (Re) is small (typically <1) and the fluids flow without turbulence—i.e., they flow “laminarly” next to each other without mixing other than by diffusion.⁷⁰ Because the fluid velocity is slower next to the walls, molecules that happen to flow closer to the walls have more time to diffuse away from their original position at the inlet than do those molecules that happen to be at the center of the channel at the inlet—yielding what is known as the *butterfly effect*,^{71,72} which consists of an apparent broadening of the diffusing concentration profile at the microchannel walls. We note that surface area is another factor that becomes important at the microscale. When going from the macroscale to the microscale, the surface-area-to-volume ratio can increase by orders of magnitude.

Compared to traditional (“macro”) cell culture fluid-handling methods, microfluidic systems are advantageous, because (1) they consume small quantities of precious/hazardous reagents; (2) they can be straightforwardly integrated with other microfluidic devices; (3) they can be mass-produced in low-cost, portable units; (4) their dimensions can be comparable to or smaller than a single cell; (5) because of the nature of laminar flow in microchannels, modeling of fluid flow velocity profiles, pressures and diffusion is straightforward; and (6) subcellular delivery of fluids is possible using multiple laminar flow streams.

Using laminar flow in a network of microfluidic channels, Takayama et al.⁷³ were able to pattern cells, cell substrates, and cell culture media. An especially interesting application of this method is to stimulate only subcellular domains of single cells with multiple parallel laminar fluid flows.^{74,75} Here, the interface between adjacent liquid streams is positioned over a single living cell so that different regions of the cell are exposed to different streams, allowing for treatment of subcellular domains of the cell. Using this technique, they were able to label different subpopulations of mitochondria with different fluorescent markers, disrupt selected regions of the cytoskeleton with the membrane-permeant drug latrunculin, digest ECM proteins on limited areas of cell-substrate adhesions with trypsin (see Fig. 4), or observe microcompartmental endocytosis within individual cells.

FIGURE 4. Microfluidic delivery of soluble factors to cells.

An example using PARTCELL (partial treatment of cells using laminar flows) to digest a portion of extracellular matrix protein underlying a bovine endothelial cell. **(A)** Schematic of the experiment. A stream of trypsin/EDTA-containing medium flows side by side with regular medium inside a microchannel, resulting in the partial detachment of the cell. **(B)** Cell before treatment with trypsin/EDTA. **(C)** After several minutes of trypsin treatment. The left side of this cell was treated with trypsin. The white dotted line indicates the approximate position of the interface between laminar flow paths with and without trypsin; this region was determined by doping the trypsin solution with fluorescent dextran. Cell surface proteins and extracellular matrix (ECM) proteins adsorbed to the channel floor were proteolytically cleaved in the treated region, and the cell detached from the substrate specifically in the trypsin-treated part; the untreated region was not affected. (Contributed by Takayama, adapted from Ref. 75.)



V. BIOLOGY ON A CHIP BY CELL TYPES

V.A. Fibroblast Biology on a Chip

Fibroblasts are cells in connective tissues that secrete collagen and take part in wound healing. The first micropattern of cell adhesiveness was produced by Carter⁷⁶ to observe the haptotaxis (contact guidance) of fibroblasts. Carter's micropattern consisted of cell-adhesive palladium (Pd) microislands on a cell-repellant cellulose acetate film created by evaporating metal through a nickel stencil mask. The applications of microfabrication in fibroblast biology presently encompass basic studies of cell adhesion, spreading, motility, proliferation, and differentiation, as well as cellular assays and tissue engineering. The most active research areas are reviewed below.

1. Effect of Microtopography on Fibroblast Behavior

In vivo, cells are surrounded by a 3-D scaffold of various ECM proteins and proteoglycans that display complex topographical micro- and nanostructures. Thus, it is important to understand how cell behavior varies with varying microtopographies and to investigate whether this knowledge can be used for designing efficient matrix scaffolds for tissue engineering.

Interested in the biocompatibility and performance of dental implants, Brunette's group⁷⁷⁻⁸⁰ has extensively studied topographic guidance of cultured human gingival fibroblasts on titanium-coated micromachined silicon wafers or epoxy replicas. Fibroblast aligned both within the micromachined grooves and on the intervening flat ridges and transmission electron microscopy showed that the cellular cytoskeleton oriented in the same fashion.⁷⁷ Using immunocytochemistry techniques, they examined the sequence of alignment of microtubules, focal contacts, and actin-filaments in fibroblasts spreading. Microtubule was the first element to align.⁷⁸ Cells with intact microtubules aligned faster and to smaller topographic features than did cells treated with the microtubule inhibitor colcemid. However, in the absence of microtubules, kinesin localized to some of the aligned stress fibers and to leading edges of cells spreading on grooves. Thus the grooved substratum compensated for the microtubule deficiency by organizing and maintaining an aligned actin filament framework.⁷⁹ Further experiments showed that the dimensions of the grooves influenced the kinetics of cell alignment. An unexpected finding was that very narrow (0.5 μm wide and 0.5 μm deep) grooves aligned cells deficient in actin microfilament bundles (cytochalasin B-treated) better than untreated control cells but failed to align cells deficient in microtubules (colcemid-treated). Thus, the microtubule system appeared to be the principal but not the sole cytoskeletal substratum-response mechanism affecting topographic guidance of human gingival fibroblasts.⁸⁰

Wojciak-Stothard et al.⁸¹ investigated the role of the cytoskeleton proteins in the spreading, elongation, and orientation of baby hamster kidney (BHK) fibroblasts to ridge and groove substratum topography and derived a different conclusion. They observed F-actin condensations close to the intersection of the wall groove and ridge top, 5 minutes after cell attachment. Vinculin arrangement at the early stages of cell spreading was similar to that of actin. Organization of the microtubule system followed later, becoming obvious at about 30 minutes after cell plating. These results supported the theory that cells react to topography primarily at lines of discontinuity in the substratum. They concluded that the aggregation of actin along groove/ridge boundaries is a primary driving force in determining fibroblast orientation on microgrooved substrata.

Clark et al.⁸²⁻⁸⁴ compared the alignment of BHK fibroblasts with that of other cells (rabbit neutrophils, epithelial MDCK cells, and chick embryo cerebral neurons) on gratings made of fused quartz with feature sizes ranging from 0.13 μm to 25 μm and found that the influence of topography is dependent on cell type, on cell/cell interactions, and on the geometry of the micropatterns. Neutrophils were unaffected by gratings. While all gratings aligned BHK cell populations, the degree of alignment was dependent on the depth and the pattern period. Single MDCK cells aligned to all patterns, their elongation being depth and period dependent, whereas colonies were mainly unaffected. The outgrowth of neurites from chick embryo neurons were mainly unaffected by the grating surfaces.^{85,86} Meyle et al.⁸⁷ also analyzed the orientation of human fibroblasts, gingival keratinocytes, neutrophils, monocytes, and macrophages on the same regular surface microstructure of 1 μm pitch and 1 μm depth. Contact guidance could not be observed in the experiments with keratinocytes and neutrophils, but 100% of the fibroblasts and approximately 20% of the monocytes and macrophages reacted with alignment. After 2 hours, some of the macrophages extended long dendritic cellular processes parallel to the long axis of the microstructures.

Control of surface topography using microfabrication has potential applications in tissue engineering. Van Kooten et al.⁸⁸ studied the effect of topology on proliferation of human skin fibroblasts on 0.5- μm -deep grooved PDMS substrates. Cells on smooth surfaces with no grooves went faster into S phase than cells on microtextured surfaces, and proliferation was slower on 10- μm -wide grooves than on 2- μm or 5- μm ones. Besides the basic percentages of cells in the different cycle phases, DNA profiles were also influenced by incubation time and texture, especially with respect to the presence of hypodiploid populations and asymmetry of the G_0/G_1 peak. This finding supported that capsule formation can be significantly reduced by using materials with textured surface elements in the micron range, an important issue in the biocompatibility of soft tissue implants. Wojciak-Stothard et al.⁸⁹ demonstrated that use of multiple grooved substrata could promote tendon healing in vitro. Epitenon fibroblasts isolated from the surface of rat flexor tendons were shown to remain more

elongated and better aligned to the groove direction than BHK cells. Epitenon cells also moved faster on patterned substrata than on plain substrata. In result, tendons cultured on multiple grooved substrata with 5- μm -deep grooves healed with complete restoration of the epitenon layer and reconstitution of the internal structure of collagen fibers; by comparison, tendons cultured on plain substrata exhibited partial healing with incompletely sealed epitenon layers and immature thin collagen fibers.

To study cell contact guidance in simultaneous presence of a topographic and an adhesive cue, Britland et al.⁹⁰ presented BHK fibroblasts with grooves of various depths (0.1, 0.5, 1.0, 3.0, and 6.0 μm deep) together with pitch-matched aminosilane tracks of various widths (5, 12, 25, 50, and 100 μm wide) at parallel and orthogonally opposed directions. They found that cell alignment was profoundly enhanced on all surfaces that presented both cues in parallel; cells were able to switch alignment from ridges to grooves, and vice versa, depending on the location of superimposed adhesive tracks; cells aligned preferentially to adhesive tracks superimposed orthogonally over grooves of matched pitch, traversing numerous grooves and ridges. Confocal fluorescence microscopy revealed two groups of mutually opposed f-actin stress fibers within the same cell, one oriented with the topographic cues and the other with the adhesive cues; however, the adhesive response was consistently dominant. This demonstrated that cells were able to detect and respond to multiple guidance cues simultaneously and that the adhesive and topographic guidance cues were capable of interacting both synergistically and hierarchically to guide cell orientation.

2. Relationships Between Cell Shape and Cell Function

Ireland et al.⁹¹⁻⁹³ studied the shape, cytoskeleton, adhesion, and behavior of Swiss mouse 3T3 fibroblasts cultured on micropatterned adhesive islands. Cell-adhesive islands of various sizes and shapes were made by evaporating palladium through a metallic stencil onto an underlying nonadhesive surface. Cell spreading was limited because focal contacts were restricted to the palladium, but single isolated cells could be stimulated to proliferate in the islands of 500–5000 μm^2 as freely as in ordinary cultures. Circular islands of area $\leq 2000 \mu\text{m}^2$ constrained cell shape and caused focal contacts and actin microfilament bundles to accumulate at the periphery of the circle—especially in islands of about 1000 μm^2 , in which a complete ring of adhesion sometimes formed in the periphery of the cell.^{91,92} Different shapes of islands caused differences in the arrangement of the cytoskeleton and in the area needed to induce a particular amount of vinculin localization. Linear islands (3- μm -wide strips of palladium) induced the same amount of vinculin localization as circles or triangles of an area three times larger. Linear islands could induce the same amount of growth as circles of triple area, supporting the notion that focal contact might act as the anchorage stimulus to growth.⁹³

The microtopography of the substrate could indirectly alter cell functionality at the genetic level via changes in cell shape. Brunette's group⁹⁴ found that fibroblast cell functions (fibronectin mRNA level, mRNA stability, and protein secretion) were related with cell shapes using microgrooved surfaces. Cells on grooved surfaces were significantly elongated and oriented along the grooves of the substratum, while cell height was approximately 1.5-fold greater than that of cells on smooth surfaces. The grooved surface increased the amount of fibronectin mRNA/cell and the amount of secreted fibronectin protein on the grooved surface, while the mRNA levels of the housekeeping gene glyceraldehyde-3-phosphate dehydrogenase were constant. The stability of fibronectin mRNA was also dependent on surface microtopography.

3. Measurement of Mechanical Forces Between Cells and ECM

Fibroblasts have been used as a model for cell adhesion and motility studies. Investigators have measured mechanical forces between cells and their underlying substrate by measuring the deformations of the substrate. Those forces are crucial for cell adhesion and locomotion.

Microfabrication was not required for the early studies of cellular force measurements. Harris et al.⁹⁵ first cultured explants and dissociated cells on a thin layer of silicone substrates (made by brief exposure of uncured PDMS to a flame, which only crosslinked its outmost layer). Other polymers such as phenylmethyl polysiloxane⁹⁶ or polyacrylamide,^{97,98} whose stiffness can be easily changed by adjusting the degree of cross-linking, have also been used. As fibroblasts migrate, the traction forces stretch and distort the substratum, producing pronounced wrinkles in the rubber that could be used as an indicator of the traction force.^{95,96} The traction force can also be more quantifiably monitored from the displacement of sprinkled or embedded fluorescent beads.⁹⁶⁻⁹⁹

Microfabricated sensors have enabled more precise measurement of traction forces and measurement of subcellular tractions generated by individual adhesive contacts. Galbraith and Sheetz¹⁰⁰ produced a micromachined device containing 5904 pads, ranging in area from 4 to 25 μm^2 , each resting on a pedestal at the free end of cantilever levers of various lengths that are buried beneath the silicon surface. When cells locomote over one pad, the forces that the cells exert on the pad can be determined by measuring the displacement of the pad and calculating the product of the pad displacement and the stiffness of the cantilever lever. The researchers found that the front of migrating fibroblasts produced intermittent rearward forces, whereas the tail produced larger forward-directed forces. All the forces had periodic fluctuations. It is interesting that the transition between forward and rearward traction forces occurred at the nucleus. It was proposed that the coupling of lamella extensions to fluctuating rearward tractions in front of the nuclear region moved the

front of a fibroblast forward, while force-facilitated release of rear adhesive contacts and anterior-directed tractions allowed the region behind the nucleus to advance. This microdevice allows for dynamic measurements of subcellular traction; however, only the projection of the force along one axis can be measured.

Balaban et al.¹⁰¹ developed a simpler method for real-time, high-resolution measurements of forces applied by cells at single adhesion sites. The method combined micromolding of elastomer substrates (PDMS) and simultaneous fluorescence imaging of single focal adhesions in live cells expressing GFP-tagged vinculin. The cells were seeded on a microtextured PDMS surface containing 0.3- μm -deep posts (*micromarkers*) that was coated with fibronectin prior to seeding. Local forces were measured by monitoring the displacement of the PDMS micromarkers (instead of randomly dispersed beads as in previous studies). They found that local forces are correlated with the orientation, total fluorescence intensity, and area of focal adhesions, indicating a constant stress of $5.5 \pm 2 \text{ nN}/\mu\text{m}^2$. The dynamics of the force-dependent modulation of focal adhesions were characterized by blocking actomyosin contractility and were found to be on a timescale of seconds.

Tan et al.¹⁰² used a similar approach with taller PDMS posts, such that the cell would bridge the posts and the posts would bend independently, hence directly reporting the subcellular distribution of traction forces. Furthermore, fibronectin was microstamped onto selected posts, causing cells to attach only onto the fibronectin-topped posts. Local substrate stiffness could be varied (from 1600 to 2.7 $\text{nN}/\mu\text{m}$) by varying the diameter and height of the elastomeric microposts in the microfabricated arrays. With this method, the authors reported two classes of force-supporting adhesions that exhibited distinct force-size relationships. Force increased with size of adhesions for adhesions larger than $1 \mu\text{m}^2$, whereas no such correlation existed for smaller adhesions. It is important to note that cell morphology regulated the magnitude of traction force generated by cells. Cells that were prevented from spreading and flattening against the substrate did not contract in response to stimulation by serum or lysophosphatidic acid, whereas spread cells did. Contractility in the unspread cells was rescued by expression of constitutively active RhoA. Together, these findings demonstrate a coordination of biochemical and mechanical signals to regulate cell adhesion and mechanics.

Another powerful and sensitive method to monitor the kinetics of cell attachment and cell motion is the electrical measurement by impedance analysis. Giaever and Keese¹⁰³ cultured the fibroblast cell lines WI-38 and WI-38 VA13 on gold microelectrodes carrying weak AC currents and measured a large change in electrical impedance when cells attached and spread on the electrodes. When the impedance was tracked as a function of time, fluctuations were observed that were a direct measure of cell motion. Surprisingly, these fluctuations continued even when the cell layer became confluent, a manifestation of cell motility that was dubbed *micromotion*. In a modified method, the experimental technique (referred to as elec-

tric cell-substrate impedance sensing, or ECIS) was optimized to demonstrate that higher-frequency capacitance measurements ($f = 40$ kHz) were better suited for following the increase in surface coverage of the electrode due to cell spreading.¹⁰⁴ Using ECIS, the attachment and spreading kinetics of epithelial MDCK cells were studied on different protein coatings. The authors quantified the inhibitory effect of soluble peptides that mimic the recognition sequence of fibronectin and other extracellular matrix proteins (RGDS). They also applied the ECIS technique to monitor the detachment of confluent fibroblastic cell layers (WI38/VA-13) following bath application of these peptides.

Hagedorn et al.¹⁰⁵ cultured mouse fibroblasts on perforated Si membranes (3 μm thick, pore diameter approximate to 10 μm , etched by KOH) and measured the impedance of the growing cells simultaneously with time-lapse microscopy of cell motility. Compared to metal surfaces, Si is inert and no charge transfer reactions occur; cells could penetrate the pores, and the pore areas were transparent, allowing for optical monitoring of the cells. The number, size, and position of pores can be precisely controlled. The method was sensitive enough to record movement of filopodia structures beyond optical microscopy resolution.

V.B. Neuronal Cell Biology on a Chip

Neuronal cell cultures, despite consisting of an environment void of most of the cell/cell communication processes that embody the higher functions of the brain such as learning and memory, provide a simplified system that can be useful in understanding basic neuronal mechanisms. One should likely dismiss the notion that it is possible to produce a “brain on a chip”—planar neuronal networks with information storage/processing capability—yet well-defined networks (i.e., where the relative position of cells and their axons/dendrites are determined by artificial design) could give valuable insights into the effect of cell/cell communication on basic processes (such as synapse development, synaptic transmission and potentiation), certain cell pathologies, and drug efficacy. For example, neuron micropatterns in combination with microfluidic devices may allow for the arrangement of cells on surfaces of sensor devices (e.g., microelectrode arrays that detect the electrical activity of a large number of neurons) used in environmental control and drug screening.

1. Micropatterning, Substrate-Cell Interaction and Contact Guidance of Neurons

The two major cell types in the nervous system are neurons and glial cells. Neuronal adhesion and axon outgrowth are guided in part by contact factors (ECM proteins

and cell adhesion molecules) in vivo and in vitro. Various micropatterning techniques have been employed to control the adhesion (and polarization) of neurons.

In 1975, Letourneau¹⁰⁶ made the first neuronal micropattern. To create a surface with differential adhesiveness, Pd was deposited through standard metal grids—commercially available for electron microscopy (EM), essentially equivalent to Carter's nickel stencil but more readily obtainable—onto polyornithin- or collagen-coated surfaces. Chicken E8 dorsal root ganglion (DRG) neurons preferred polyornithin or collagen over Pd. Cooper et al.¹⁰⁷ vacuum deposited thin films of silicon monoxide through masks and found that mouse neuroblastoma cells NB41A adhered and neurites aligned on the silicon monoxide lines. Hammarback et al.¹⁰⁸ created micropatterns of “bioactive” and inactive laminin by ultraviolet light inactivation of laminin-coated coverslips masked with EM grids; they found that axon growth cone guidance of chicken embryonic DRG neurons by substrate-bound laminin pathways was correlated with neuron-to-pathway adhesivity.¹⁰⁹ By UV irradiation of agarose/albumin surface through EM grids followed with laminin absorption on the irradiated region, they also created patterns of laminin-coated (high adhesivity) surfaces interspersed with agarose/albumin (low adhesivity)-coated regions.¹¹⁰ Neurons only adhered to the laminin-coated regions, but some neurites extended across intervening agarose/albumin regions, supporting the guidepost hypothesis for pioneer axon pathfinding. Gundersen^{111,112} patterned nerve growth factor (NGF), laminin, or fibronectin on coverslips with micropipettes and cultured chick embryonic DRG explants on the patterned surface. Adsorbed NGF and laminin, but not fibronectin, guided the direction of neurite elongation.

Kleinfeld et al.¹⁰ first produced high-resolution micropatterns of dissociated neurons on photolithographically patterned glass substrates. Selective attachment and growth of neurons (either embryonic mouse spinal cells or perinatal rat cerebellar cells) was accomplished by creating a micropattern of alternating aminosilane SAM and alkylsilane SAM regions. Although the selectivity was attributed to a higher hydrophobicity of the alkylsilane regions, it is unlikely that the neurons could “see” the end-terminal groups of the SAMs because the cells were cultured in medium containing serum (5–10%). Nevertheless, neurons were confined to square regions on the scale of 50 μm or on lines with widths less than 10 μm . The patterned growth of cerebellar cells was maintained up to 12 days in vitro; granule cells and Purkinje neurons developed normal electrical excitability. Glial cells were also patterned along with the associated granule cells indicated by glial fibrillary acid protein (GFAP) immunostaining.

Since then many studies in neuronal patterning have been performed in a variety of labs, using various methods, including surface modification by silane chemistry,¹¹³⁻¹¹⁶ photolithography,^{113,114,117-119} deep-UV lithography,¹²⁰⁻¹²² excimer laser ablation,^{123,124} soft lithography,^{24,125-129} oxygen plasma etching,^{117,130,131} biospecific peptide immobilization,^{122,132-137} and physi- or chemisorption of poly lysine,^{24,124-}

^{126,128} laminin, ^{108,127,138,139} or polylysine-conjugated laminin ¹²⁹ on various substrates including Si, gold, silicone, glass, ^{24,116,118,122,124,125,138} glassy carbon, ¹³⁷Ti, ¹⁴⁰ polystyrene, ^{130,131} Teflon (fluorinated ethylene propylene), ^{132-134,141-144} and biodegradable polymers.¹⁴⁵ These studies mainly yielded insights into the adhesion and guidance of neuronal growth by insoluble factors and could prove valuable for selective neuronal immobilization on future microsensors.

A long-standing hurdle in creating well-defined neuronal networks is that of the polarity of neurons. Neurons have many inputs and an output, and reproducible studies concerning large ensembles of neurons would have to control not only where the cell bodies attach but also the direction in which the inputs and the output grow. A report by Stenger et al.¹⁴⁶ deserves special mention because it demonstrated the control of the polarity of embryonic hippocampal neurons in a specified direction by means of (adhesive) aminosilane SAM patterns on a (nonadhesive) fluoroalkylsilane SAM background (despite the difficulties in controlling protein physisorption from the medium onto SAMs). Cell bodies adhered to a 25- μm -diameter island and had the alternative of extending processes along four 5- μm -wide paths in orthogonal directions, with the particularity that three of the paths were interrupted in 10- μm -long segments, whereas the fourth one was continuous. Most of the cells grew their axon along the continuous path and dendrites along the other three paths, as identified by immunostaining of process-specific markers (microtubule-associated proteins and neurofilament polypeptides). This result shows that there is an intrinsic mechanism that determines cell polarity as a function of surface signals.

The branching morphology of neurons also appears to be influenced by micropatterned substrates. Clark et al.¹⁴⁷ found that DRG neurons were multipolar with highly branched neurites on planar substrata but were typically bipolar with reduced or absent neurite branching on 25- μm laminin tracks. These observations suggest that substrata might regulate the precision of growth cone advance and that patterned adhesiveness might play a role in neuronal morphological differentiation.

In vivo neurons are also guided by the 3-D topography of their environment. For tissue engineering applications, the micron-scale geometry of the surface of regeneration guidance channels influences the outcome of peripheral nerve regeneration, potentially by affecting the early arrangement of the fibrin matrix and/or inducing different cellular responses.¹⁴⁸ Nagata et al.¹⁴⁹ cultured dissociated neuroblasts on quartz plates with grating-like microstructures fabricated by lithographic techniques. Various types of CNS neuroblasts, but not PNS neurons, oriented their processes and migrated both perpendicular and parallel to the axis of the microstructure. Perpendicular orientation was frequently observed when the microstructured grooves had depths between 0.3 μm and 0.8 μm and a width of 1 μm , which roughly mimics a tightly aligned neurite bundle. Rajnicek et al.¹⁵⁰ cultured dissociated embryonic *Xenopus* spinal cord neurons and rat hippocampal neurons on quartz etched with a series of parallel grooves. *Xenopus* neurites grew

parallel to grooves as shallow as 14 nm and as narrow as 1 μm ; on the other hand, rat hippocampal neurites grew parallel to deep, wide grooves (130–1100 nm deep, 4 μm wide) but perpendicular to shallow, narrow ones (14–520 nm deep, 1 μm wide). The frequency of perpendicular alignment of hippocampal neurites depended on the age of the embryos from which neurons were isolated, suggesting that contact guidance is developmentally regulated. The perpendicular alignment persisted in the presence of the stretch-activated calcium channel blocker gadolinium chloride, the G protein inhibitor pertussis toxin, the protein tyrosine kinase inhibitor genistein, the protein kinase A and G inhibitor HA1004, the protein kinase A inhibitor KT5720, or the protein kinase G inhibitor KT5823. Low concentrations of the protein kinase C inhibitors staurosporine, bisindolylmaleimide, or H-7 did not affect perpendicular orientation, but higher concentrations inhibited it. The calcium channel blockers flunarizine, nifedipine, and diltiazem also inhibited perpendicular orientation. Influx of calcium and protein kinase C activity therefore appeared to be involved in perpendicular contact guidance.¹⁵¹

In vivo growth cones are required to make complicated navigational decisions when different guidance cues are encountered simultaneously. Putative candidates for steering growth cones are soluble tropic molecules, topographic features of the environment, ECM adhesion molecules, and endogenous electric fields. In our study of axon guidance (see Fig. 5), we have micropatterned mouse embryonic cortical neurons with adhesive cues (polylysine or laminin) surrounded by nonadhesive substrates (polystyrene, glass, and interpenetrated networks of the copolymer PIAAm-co [PEG IPN]). Figure 5A shows a cortical explant attached to a set of polylysine lines on glass; the neurons in the slice preferred to grow processes along the polylysine lines over the bare glass areas, concurring with earlier findings. The dissociated neurons shown in Figure 5B are growing processes within a polylysine-coated circle in a nonadhesive background of PEG IPN. The pattern was created by selective etching of a homogeneous PEG IPN layer through a PDMS stencil.²⁸ When constrained to this pattern for long periods of time (Fig. 5C, 21 days), the neurons will eventually reach to neighboring islands and join their axons in bundles. In the absence of differential contact guidance cues, the surface topography of a PDMS substrate (uniformly coated with an adhesive factor) can also guide the growth of axons (Fig. 5D). Control of the initial growth direction of axons by contact guidance should provide a robust assay for studying combinatorial effects of soluble and contact axon guidance factors.

Britland and McCaig¹⁵² studied the integrated responses of embryonic *Xenopus* spinal cord neurons to simultaneous electrical and adhesive guidance cues. Neurons were growing on a photolithographically micropatterned laminin substrate with an orthogonal DC electric field. Normally, application of a DC field to growth cones immediately induced filopodial asymmetry and caused the growth cone to turn and orient cathodally. However, on micropatterned laminin tracks after the application

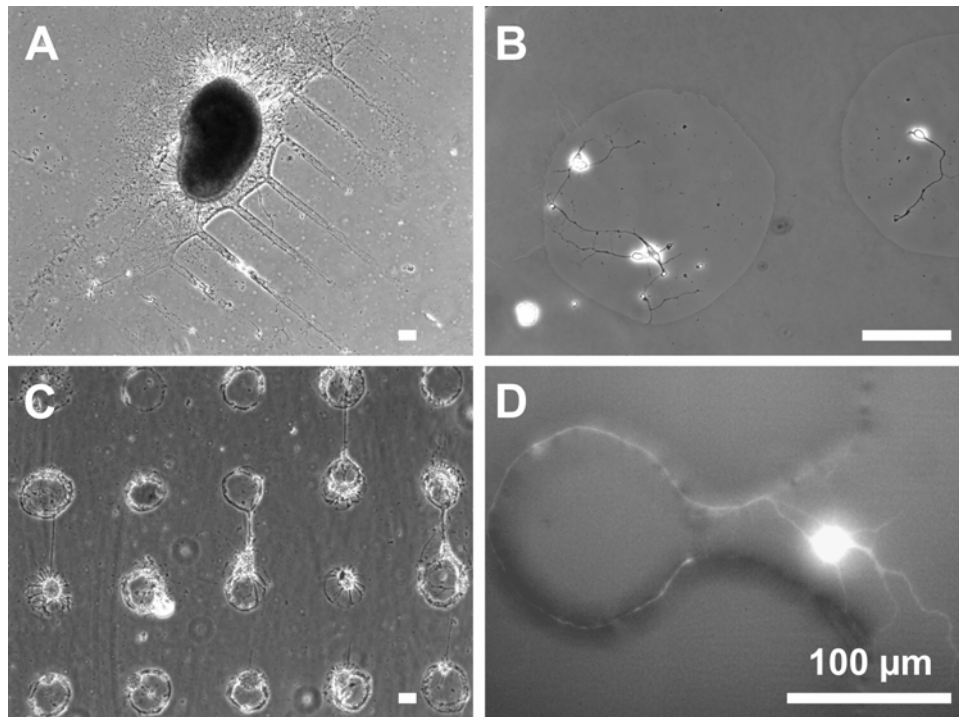


FIGURE 5. Contact guidance of neuronal growth with various soft lithographic techniques. Phase microscopy images from Folch lab showing contact guidance of mouse embryonic cortical neurons with surface protein patterning and surface topography. **(A)** A cortical explant (E16, 12 DIV) grown on microfluidically-patterned PDL lines on a glass coverslip. The explant initially attached to the nonpatterned PDL area, and then the neurites extended to patterned areas and aligned on the PDL lines. **(B)** PDMS stencils, in combination with selective etching of PEG IPN, provided a more precise means to position neurons. Note that neurons (E13, 3 DIV) only attached and grew inside the PDL-coated, PEG-IPN-surrounded circles, but rarely extended to the PEG IPN areas (note the edge of the circles). **(C)** PEG IPN patterns enabled long-term patterning of neurons. The image shows neurons at 21 DIV still confined in the PDL-coated islands; however, neurite bundles formed between islands. **(D)** An example of axon growth guided by surface topographical features on PDMS substrates. Neurons were loaded with a live cytoplasmic dye to better view the neurites. Neurons grew inside recessed PDMS wells (E13, 3 DIV). The PDMS surface was uniformly coated.

of a 100–140 mV/mm DC field, the majority of cells remained aligned with the laminin tracks. A proportion of aligned neurites oriented cathodally, and evidence of a response to both directional cues was even found within the same cell. Furthermore, cathodal orientation in *Xenopus* growth cones was reversed if laminin tracks

were replaced with polylysine. This suggests that growth cones are able to detect and integrate at least two morphogenetic guidance cues simultaneously.

Although neuronal growth can be patterned according to adhesiveness of substrates, there appeared to be a difference between permissive versus instructive influences. Buettner and Pittman¹⁵³ systematically measured several features of outgrowth by dissociated neonatal rat sympathetic neurons on different concentrations of laminin ranging from 0.01 to 1.0 $\mu\text{g}/\text{cm}^2$ and found that neurite outgrowth parameters were relatively insensitive to changes in laminin concentration. Lemmon et al.¹⁵⁴ examined neurite growth rates, the degree of neurite fasciculation, the choices neurites make between two substrates, and the relative adhesiveness on different substrates. They found that the relative adhesiveness of a substrate was a poor predictor of either axon growth rate or the degree of fasciculation. Furthermore, neurites showed little selectivity between three different naturally occurring substrates: L1, *N*-cadherin, and laminin. These results indicate that some adhesion molecules may serve as permissive substrates, in the sense that they can define axonal pathways, but they do not provide information about which path to take at a choice point or about which direction to go along the path; in addition, substrates *in vivo* may not exert their effects on axon guidance principally via relative adhesiveness.

Recently Dertinger et al.⁶⁸ studied the influence of laminin *gradients* on neuronal guidance. Complicated gradient shapes could be created on poly L-lysine-coated PDMS substrates using microfluidic patterning with a soluble-gradient-generating device. Without microfabrication technology, it would be very difficult to fabricate gradients over the distances required for biological studies (a few hundred microns). Rat hippocampal neurons were cultured on these substrate-bound gradients. When compared to axons growing on a homogeneous laminin layer, axons growing on laminin gradients showed a preference to orient toward the direction of increasing surface density of laminin. Linear gradients in laminin adsorbed from a gradient in solution having a slope of laminin concentration larger than $\sim 0.06 \mu\text{g}/(\text{mL} \times \mu\text{m})$ (defined by dividing the change of concentration of laminin in solution over the distance of the gradient) oriented axon specification, whereas those with laminin concentration smaller than $\sim 0.06 \mu\text{g}/(\text{mL} \times \mu\text{m})$ had no effect.

2. *In Vitro* Neuronal Networks

Although various micropatterning techniques have been widely used in patterning neurons in culture, it is worth noting that to date neuronal growth is not sufficiently well understood to yield reliable and functional connections at the extremely low local densities inherent in such networks, because most neurons do not divide after terminal development. Only a few reports have demonstrated the electrophysiological characterization of a neuronal network.

Jimbo et al.¹⁵⁵ simultaneously monitored intracellular calcium with Fluo-3 and electrical activity with extracellular electrode arrays from patterned neural networks in culture. Under low magnesium conditions, cultured rat cortical neurons showed periodic transients of Fluo-3 fluorescence synchronized with the recorded periodic electrical bursting, indicating that functional synaptic connections were formed in the culture system.

Ravenscroft et al.¹⁵⁶ produced high-resolution (2–20 μm) organosilane patterns and reported the guidance of neuronal adhesion and neurite outgrowth and the formation of reproducibly defined circuits of embryonic (E18–19) rat hippocampal neurons on these patterned surfaces in vitro (>50% pattern compliance). The authors monitored synaptic development (spontaneous and evoked postsynaptic currents [sPSCs and ePSCs]) of selected neurons using dual patch-clamp electrophysiology, but a full characterization of the network was not possible with this recording technique.

Ma et al.^{157,158} compared synaptic formation of cultured embryonic hippocampal cells on trimethoxysilylpropyl–diethylenetriamine (DETA), 13F, or DETA/13F patterns with surfaces coated with uniform poly D-lysine. With immunostaining for synapsin I and microtubule-associated protein-2 (MAP-2) and dual patch-clamp of sPSCs and ePSCs, they found that fully functional synapses were formed on DETA surfaces similarly to polylysine-coated surfaces. MAP-2 positive neuronal soma and rapidly growing dendrites were co-localized with synapsin I puncta faithfully along DETA lines. Synapsin I, MAP-2, and sPSCs emerged together at days 3–4 and increased at day 7, when ePSCs appeared. Synaptic signals occurring during 4–7 days in culture were all GABAergic.

3. Extracellular Electrode Arrays for Multisite Recording and Stimulation of Neurons

To monitor the activity of in vitro neuronal networks, long-term, noninvasive recording or stimulation of neuronal electric activity is needed. Extracellular recording by single field effect transistors (FETs)¹⁵⁹ as well as arrays of FETs¹⁶⁰ has been shown. In this configuration, neurons “sit” on the non-metallized gate of the FET, affecting the source–drain current by capacitive coupling when the neuron undergoes a membrane voltage change. Capacitive stimulation of neurons with FETs can also be achieved.¹⁶¹ Multiple electrode arrays (MEAs) of up to 100 electrodes patterned by photolithography on glass or silicon substrates have been used for decades; transparent MEAs can be made of indium tin oxide.^{162,163} Planar MEAs, consisting of 10–100 electrode sites (with diameters on the order of the cells—i.e., ranging from a few microns up to a few tens of microns) spaced at 100–200 μm interdistance on glass plates, were used by Thomas et al.,¹⁶⁴ Gross et al.,¹⁶⁵ Novak and Wheeler,¹⁶⁶

and many others followed in studies of the activity and plasticity of developing cultured neuronal networks^{167,168} or slices.^{162,163,169-173} MEAs are now commercially available in a variety of formats.

Wilkinson et al.^{174,175} used planar MEAs to study single isolated leech neurons in culture. The 100- μm^2 platinized gold microelectrodes in the 64-electrode array detected the external current that flows during an action potential with signal-to-noise ratios of up to 500:1, giving a maximum recorded signal of several millivolts. The performance of these electrodes is enhanced if good sealing of the cells over the electrodes can be obtained, and further enhanced if the electrodes and the cells lie in a deep groove in the substratum. The velocity and direction of action potential propagation were investigated by simultaneously recording on multiple sites of their long processes. Propagation from the broken stump toward the cell body (antidromic) was observed for spontaneous action potentials, action potentials produced by injecting current into the cell body, and extracellular stimulation of the extracted process via a planar extracellular electrode. These results supported previous findings that the tip of the broken stump of extracted neurons has a high density of voltage-activated sodium channels. Moreover, the findings demonstrated the applicability of extracellular electrode arrays for recording the electrical excitability of single cells.

Using a 60-electrode substrate-embedded multielectrode array, Shahaf and Marom¹⁷⁶ demonstrated that cultured neonatal cortical neuronal networks can seemingly “learn” certain tasks. The arrays used in these studies consisted of 60 Ti/Au/TiN electrodes, 30 μm in diameter, and spaced 200 μm from each other. The silicon nitride insulation layer was pretreated with poly L-lysine. The network was first focally stimulated at a low frequency (0.3–1 Hz) until a desired predefined response was observed 50 ± 10 msec after a stimulus, then the stimulus was stopped for 5 minutes. Repeated cycles of this procedure ultimately led to the desired response being directly elicited by the stimulus. This finding shows that neuronal networks may be useful for studying basic synaptic potentiation rules.

Extracellular recordings are noninvasive and allow for long-term recordings for multiple sites, but suffer from very low signal-to-noise ratios because of imprecise positioning of the cell relative to the electrode surface (both in the vertical and horizontal directions). To better define the cell-to-electrode distance, electrodes have been coated with ECM proteins,¹⁷⁷ poly lysine,^{178,179} or silane-based monolayers.¹⁸⁰ In addition, electroplating of Pt-back¹⁸¹ or coating metal electrode with electrically conductive polymers (e.g., polypyrrole)¹⁸² can be used to lower the impedance of the electrode sites. Cell positioning onto electrodes can be improved by surface micropatterning to improve the sensitivity and repeatability of MEA recordings. James et al.¹⁷⁸ microstamped poly lysine grids (1–2 μm line width) aligned to underlying MEA of Au electrodes. Rat hippocampal neurons attached and neurites extended faithfully on the poly lysine areas, thus crossing over to the electrode sites. Maher et al.¹⁸³ presented a “neurochip” to continuously and individually monitor and

stimulate cultured neurons. The device consists of a 4×4 array of metal electrodes, each of which features a caged well structure designed to hold a single mature cell body while permitting normal outgrowth of neural processes. Others have used dielectrophoretic trapping of cells as a way to position cells on the electrode sites of microelectrode arrays.^{184,185}

4. Patch Clamp Arrays for Whole-Cell or Single-Ion-Channel Recordings

The patch clamp technique¹⁸⁶ is a method that allows for the direct measurement of currents through ion channels with sub-millisecond resolution using glass micropipettes sealed against the cell membrane. Furthermore, the technique allows control of the electrical and chemical environment of a membrane and the application of signaling molecules, drugs, etc., to both sides of the membrane. However, the present patch clamp recording and stimulation technology is based on a delicate procedure that requires an experienced operator to position the glass pipette, with bulky micromanipulators under the microscope, onto the cell to obtain a “gigaohm seal,” which results in very low throughput and inability to probe many cells simultaneously. Currently, several laboratories are developing various procedures to build planar patch-clamp-on-a-chip devices, whereby cells are deposited atop a micron-sized hole on a thin insulating substrate and fill a cavity or channel underneath the cell culture surface with electrolyte solution (i.e., the hole and the cavity act as a “microfabricated, prepositioned pipette”). Schmidt et al.¹⁸⁷ made apertures (0.6–7 μm in diameter) in silicon nitride membranes (0.1–1 μm thick) suspended over a silicon pit; they used a combination of anisotropic KOH silicon etching and reactive-ion etching (RIE), followed by building SiO_2 layer with deposition and thermal oxidation. Lipid vesicles were electrophoretically positioned onto the aperture, and seals with the membrane patches could be obtained with resistances of up to 200 $\text{G}\Omega$ if the chip was coated with poly lysine or chemically modified with 4-aminobutyldimethylmethoxysilane. Pantoja et al.¹⁸⁸ reconstituted ion channels in lipid bilayers suspended in the pores of SiO_2 membranes created by RIE. Sigworth’s group¹⁸⁹ micromolded arrays of planar PDMS patch electrodes with apertures of 2–20 μm . By plasma oxidation of PDMS, they could temporarily improve the hydrophilicity of PDMS and obtain seals on oocytes expressing potassium channels. Lehnert et al.¹⁹⁰ mimicked the 3-D shape of a glass micropipette by creating micron-sized (down to 2.5 μm) hollow SiO_2 nozzles on Si/ SiO_2 wafer using photolithography, RIE, and thermal oxidation processes. Cells were reliably positioned on the nozzles by suction through the aperture and the underlying fluidic channels. Seal resistances of 100–200 $\text{M}\Omega$ was obtained on Chinese hamster ovary (CHO) cells. Unfortunately, silicon substrates are opaque, precluding microscopy observation. The first report of a gigaohm-seal recording on small mammalian cells is credited to Behrends’ group,¹⁹¹ who created geometrically

defined submicron apertures in glass substrates by ion (highly accelerated gold) track etching and were able to record from CHO cells with typical seal resistance of 1–10 G Ω . These devices also allow for recordings from ion channels on artificial lipid bilayers¹⁹² or single membrane patches¹⁹³ and from single ion channels.¹⁹⁴ Unfortunately, although glass patch-on-a-chip devices are the most promising ones due to the similarity with micropipettes in surface, the particle accelerator required for ion track etching is not available in most research institutions.

5. Microfluidic Delivery of Factors to Neurons

Microchannels can be used to selectively deliver soluble factors to neurons. Recently, Taylor et al.¹⁹⁵ created a neuron culture PDMS device with the capability to direct neuronal attachment and neurite outgrowth and to fluidically isolate compartments within the culture area. Essentially, the device consisted of two chambers interconnected with a set of 120 parallel PDMS microchannels 10 μm in width, 3 μm in height, and 150 μm in length. Poly lysine patterning facilitated the directed growth of the neurites. As neurons (initially seeded only in one chamber) grew neurites into the other compartment through the microchannels over 3–4 days, the part of the neurites in the second chamber was effectively in a different fluidic compartment that could be perfused independently of the somal chamber. Because of the high fluid flow resistance of the microchannels, chemical stimuli could be applied to and contained in only the neuritic compartment if the somal compartment was kept at a slightly higher pressure by transferring a small volume (~ 10 – $30 \mu\text{L}$) of medium from the neuritic compartment to the somal compartment. The authors demonstrated the selective loading of dendrites with Calcein AM and Texas Red Dextran without appreciable leakage into the soma compartment for over 15 hours. Compared to laminar-flow delivery of fluids with subcellular resolution,⁷⁴ this method does not have the complications associated with maintaining flow for long periods of time, but it does not allow for relocating the interface between the two fluids at will.

6. Neuron-Based Biosensors

Biosensors integrate a biological sensing element (such as a receptor or an enzyme) to convert an environmental change (e.g., the appearance of a binding factor) into signals conducive to processing. Presently, the majority of sensor and diagnostic technologies use binding components such as antibodies, nucleic acids, or protein ligands—immobilized molecules that act as “biological affinity” sensors. However, because the sensing molecules are not in their native state, they often degrade and/or have reduced affinities. Cell-based sensors try to circumvent this problem simply

by presenting the biological affinity sensor in its native state—i.e., in/on the cell, which acts as the natural maintenance machine for the sensor. Possible applications of cell-based sensors include screening large libraries of drugs for activity or toxicity, detection and classification of emerging or engineering environmental threats, and diagnostic information from clinical samples related to diseases. Neurons have been long hailed as cell-based sensors for a variety of applications,^{196,197} but with limited success, probably because neurons are one of the most challenging cell types to culture. Gross and coworkers¹⁹⁸ pioneered the use of cultured neuronal networks on multielectrode arrays as biosensors. They used mice spinal or cortical neuronal networks for the long-term monitoring of multichannel, spontaneous, or evoked electrophysiological activity. In the absence of the homeostatic control mechanisms of the central nervous system (CNS), these networks showed remarkable sensitivities to minute chemical changes and mimicked some of the properties of sensory tissue.¹⁹⁸ These sensitivities could be enhanced by receptor upregulation and altered by the expression of unique receptors via transgenic mouse technology.¹⁹⁸ Applications of the networks included drug screening for cannabinoid agonists¹⁹⁹ and acetylcholine esterase inhibitors.²⁰⁰ Martinoia and coworkers^{168,201} simulated the signals generated by networks of neurons on microelectrode arrays (MEAs) by computer software, then employed chick embryo spinal neuron networks on MEAs and analyzed the effects of different drugs (NBQX, CTZ, MK801) on the burst activity of the “bio-electronic neuronal sensory system.”²⁰²

Compared to cell-free biosensors, cell-based biosensors face the widely underestimated challenge of cell culture maintenance—without proper control of the extracellular environment, the sensor output risks being highly irreproducible. The use of neurons has been proposed mostly for two reasons—their electrical output (making it easy to interface with electronic data processing chips²⁰³) and their relevance to neurotoxin exposure. However, both advantages are far outweighed by the monumental difficulty of maintaining neurons alive in culture, especially in a challenging environment. It is important to note that the advent of calcium imaging (allowing for optical detection at much higher throughput than achievable with microelectrodes) and heterologous expression of receptors (in more robust cell types) has reduced the usefulness of neuron-based sensors to a much narrower range of applications.

V.C. Glial Cell Biology on a Chip

Besides neurons, glial cells are a major cell type of the nervous system. Their subtypes are termed *astrocytes*, *oligodendrocytes*, and *microglia* in the CNS and *Schwann cells* in the peripheral nervous system.

In vivo, astrocytes closely wrap around neuronal synapses, provide neuronal

migration cues, act as “housekeepers” of the extracellular environment, and actively modulate neuronal activity and synaptic transmission. In pathological conditions such as injury or trauma, astrocytes often aggressively migrate to the injury site, resulting in a condition called *reactive gliosis*, which may prevent nerve regeneration and present a challenge for long-term functioning of neural prostheses.

In vitro, in serum-containing medium, astrocytes readily attach to various substrates, such as glass or plastic. As shown above, micropatterning applications require the use of a suitable cell-repellent background. One such material to repel glia adhesion is agarose. To study the growth control of human glial cell line, Westermark²⁰⁴ modified the Carter method and evaporated palladium through copper EM grids onto a thin film of agarose on tissue culture dish. Single-cell clones were obtained on the adhesive palladium islands, but cell proliferation ceased after over a week on the pattern, consistent with the notion that restriction of cell spreading leads to growth inhibition. Hydrophobic alkylsilanes may indirectly constitute another cell-repellent surface. St. John and coworkers^{205,206} studied the attachment and growth of astrocytes on silicon surfaces microstamped with patterns of DETA (hydrophilic and cell adhesive) surrounded by octadecyltrichlorosilane (OTS, hydrophobic, and cell repellent). LRM55 cells (a rat astrocyte cell line) attached selectively to DETA SAM areas with minimal attachment to OTS areas. The attachment selectivity is likely to be attributable to the presence of an intermediate layer of ECM on the silanes.

It has been shown that, besides ECM proteins, a cell/cell binding protein could be used to selectively mediate astrocyte adhesion. Synthetic peptides were covalently linked to aminosilane-modified glass coverslips using a carbodiimide-based reaction. Under serum-free conditions, cortical astrocytes, but not rat skin fibroblasts CRL-1213, exhibited enhanced adhesion onto substrates modified with KHFSDDSSSE, a peptide that mimics a homophilic binding domain of neural cell adhesion molecule (NCAM). In contrast, fibroblasts, but not cortical astrocytes, selectively adhered to glass surfaces modified with the integrin-ligand peptide RGDS.²⁰⁷

The attachment of astrocytes is also regulated by topography. Turner et al.²⁰⁸ made silicon surfaces with different textures by first producing nanometer-scale columnar structures (“silicon grass”) using a reactive ion etch followed by selectively wet etching patterned areas using standard photolithographic techniques. The astrocyte cell line LRM55 showed a preference for wet-etched regions over grassy regions. In contrast, primary cortical astrocytes from neonatal rats showed a preference for silicon grass over the wet-etched surface. The results suggest that micro-patterning and nano-texturing may be effective in controlling astrocyte interactions with implant materials for long-term implantations.^{209,210}

Intercellular signaling is critical for the normal development and physiology of the CNS. Intracellular calcium elevation in one astrocyte caused by neurotransmitters can propagate to other neighboring astrocytes and induce an intercellular calcium

wave. Takano et al.²¹¹ presented an elegant approach for studying such signaling using micropatterned glia. Micrometer-scale lines of nonadhesive agarose were microfluidically patterned onto cell adhesive poly L-lysine-coated coverslips. When primary cortical astrocytes were plated onto these substrates, confluent domains of astrocytes grew only on the poly L-lysine domains. Studies of calcium signaling revealed that astrocytes grown on such patterns retained their native physiological activity, based on the analysis of the propagation rate for calcium waves within individual astrocyte domains and across spatially disconnected neighboring astrocyte domains. Moreover, the micropatterned cultures provided a better approach for noninvasive, quantitatively dissecting extracellular diffusive messenger vs. gap-junction-mediated mechanisms of calcium wave propagation.²¹¹ As shown in Figure 6, when the extracellular ATP pathway was blocked by the P2 receptor antagonist PPADS, the calcium wave induced by mechanical stimulation were smaller in the same lane and absent in adjacent lanes, indicating that both the long-range ATP pathway and the short-range gap-junction pathway are involved in mediating normal calcium waves.

Oligodendrocyte progenitors arise in subventricular zones and migrate extensively during development before differentiating into mature oligodendrocytes, which myelinate nerve tracts in the CNS. Webb et al.²¹² microfabricated periodic contours similar to those of CNS axons to assess the influence of substratum topography on oligodendrocytes isolated from 7-day rat optic nerve. Oligodendrocytes were highly aligned by surface contours as small as 100 nm deep with 260 nm repeat spacing. Furthermore, the topographical pattern inducing maximal alignment of oligodendrocyte lineage cells corresponded to the diameters of single axons within the 7-day optic nerve, suggesting that the migration of oligodendrocyte type-2 astrocyte progenitors and axonal ensheathment by oligodendrocytes may be guided by axonal topography within the developing nerve.²¹²

In the peripheral nervous system, Schwann cells are closely associated with, and play key roles in, the development, maintenance, and regeneration of peripheral neurons. Following injury, Schwann cell orientation may also play a role in guiding regenerating axons. Detrait et al.^{131,213} patterned Schwann cells by competitive absorption of adhesive fibronectin (or collagen) and cell-repellant pluronic F68 (or albumin) onto heterogeneous polystyrene surfaces composed of oxygen plasma-treated stripes (PSox, low hydrophobicity) separated by nontreated areas (PS, high hydrophobicity). Attachment factors were adsorbed on PSox stripes, while adsorption of antiadhesive molecules on the most hydrophobic PS areas prevented cell adhesion or growth. With the right concentration and concentration ratio of fibronectin and pluronic, Schwann cells selectively attached and oriented along PSox lines.^{131,213} Thompson and Buettner²¹⁴ cultured Schwann cells on micropatterned laminin surfaces, alternating 20- μ m regions of laminin with bovine serum albumin (BSA) stripes. The Schwann cells predominantly attached and elongated on the laminin stripes and organized into multicellular aggregates that were oriented with

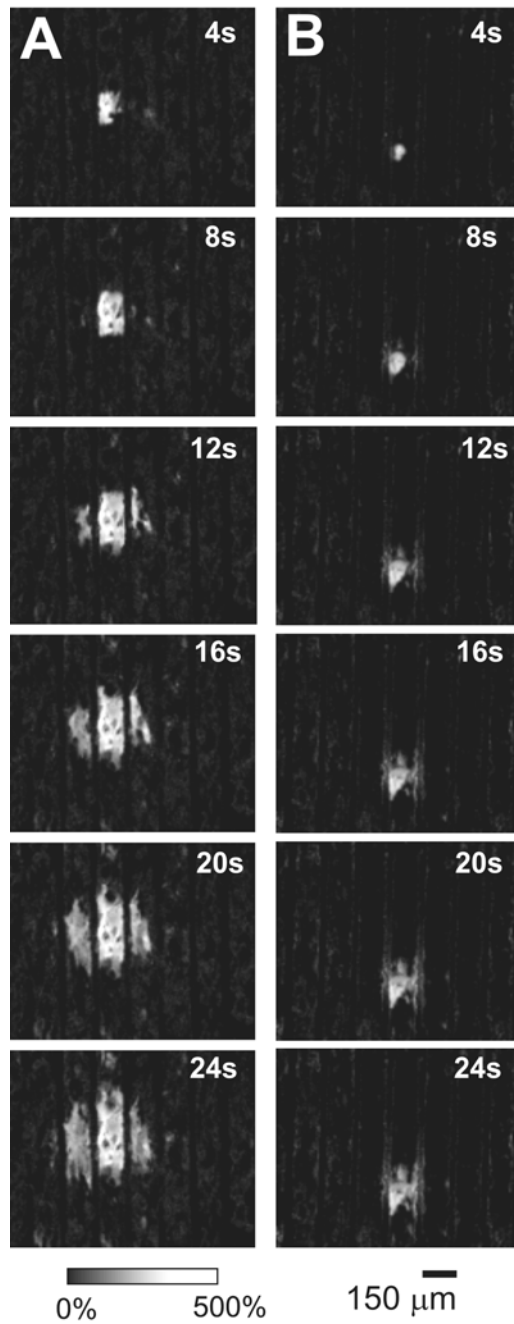


FIGURE 6. Probing intercellular communication pathways with micropatterned substrates. Two sets of fluorescence (dF/F_0) image sequences for confluent lanes of astrocytes formed on 110- μm -wide poly-L-lysine lanes that were separated by 40- μm -wide agarose films. **(A)** Sequence of images for astrocytes loaded with calcium indicator Fluo-3 AM immediately after mechanical stimulation. A calcium wave spread to astrocytes in the same lane and then to astrocytes in adjacent lanes. **(B)** Sequence of images astrocytes loaded with Fluo-3 AM and with 50 μM PPADS (an ATP receptor antagonist) present in the extracellular saline. After mechanical stimulation, the calcium wave propagated only to a few cells in the same lane, but not to adjacent other lanes, confirming a role of extracellular diffusible ATP in mediating normal intercellular calcium wave. (Contributed by Takano et al.²¹¹.)

the micropattern. The ability to control cell placement and orientation facilitates future investigations of Schwann-cell/neuronal interactions *in vitro*.

V.D. Muscle Cell Biology on a Chip

1. Micropatterns of Skeletal Myoblasts and Myotubes

In the development of muscle tissues, embryonic muscle cells (*myoblasts*) fuse to form elongated *myotubes* (multinucleated cells), and myotubes align in parallel to form highly organized myofibers with strong contractile capability. In vitro, both primary muscle cells and muscle cell lines can be induced (by serum starvation) to fuse and form myotube-like structures, but in traditional cultures the myotubes are randomly oriented, branched, and interconnected into complex structures. As early as 1983, Turner et al.²¹⁵ were able to guide the in vitro orientation of myotubes by patterning fibronectin lines on a culture dish using an ingenious “urea lift-off” method. When urea was dried, sometimes parallel or nearly parallel crystal patterns would form; when fibronectin was dried with urea, fibronectin would be deposited between urea crystals; after urea was washed out, fibronectin patterns could be formed on the culture dish. Chick embryonic myogenic cells presumably aligned on the fibronectin patterns to end up forming myotubes; unfortunately, the fibronectin patterns were far from precise or reproducible.

Clark et al.²¹⁶ micropatterned tracks of laminin (width ranging from 5 to 100 μm) absorbed on hydrophobic organosilane-treated glass and investigated the role of adhesiveness in muscle development. Myoblasts (immortal myogenic cells, H2k(b)-tsA58) adhered both to the untreated glass and to laminin on the previously hydrophobic tracks, but showed a preference for laminin: cell alignment increased upon differentiation into myotubes and continued to increase as the myotubes matured. In addition, adhesion to laminin was required for long-term survival of the myotubes, because myotubes formed on non-laminin surfaces began to detach after 2 days of differentiation.²¹⁶

In our lab, we have used selective surface modification techniques to establish 2-D spatial cues for guiding myoblast attachment, alignment, and fusion into multinucleated myotubes, in order to direct the spatial organization of the myotubes to resemble the organization found in vivo. We cultured myogenic cells (C2C12 cell line) on microtracks of physisorbed fibronectin or MatrigelTM surrounded by protein-repellent PEG IPN.²⁸ PEG IPNs repelled cell adhesion and spread robustly over a long term (>4 weeks; we have not determined the upper value). To produce cell-adhesive tracks alternating with IPNs, we first homogeneously grafted PEG IPNs onto glass substrates and then used PDMS microchannels to selectively remove IPNs with oxygen plasma and to deposit ECM proteins onto etched tracks. As shown in Figure 7, C2C12 cells adhere and spread strictly onto adhesive microtracks and responded to the spatial constraints by fusing along the track direction into spontaneously contracting, organized myotubes with width approximating the width of the adhesive lines.

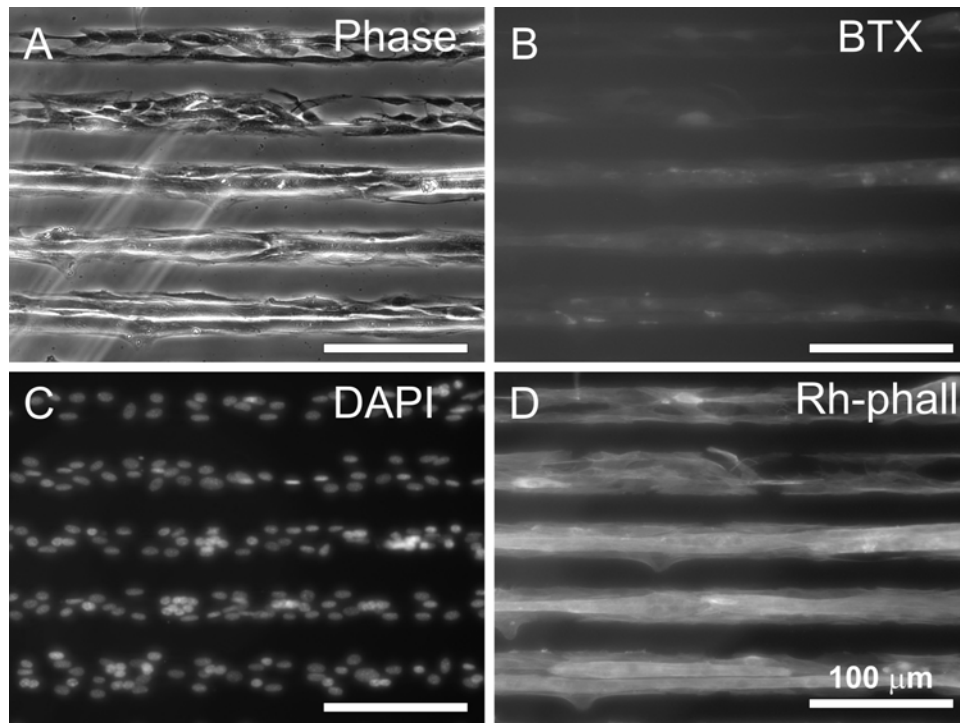


FIGURE 7. Geometrical control of muscle cell differentiation in vitro with micropatterned substrates. Muscle cells from C2C12 myogenic cell line grown on adhesive microtracks surrounded by protein-repellent background (PEG-IPN) responded to the spatial confinement by fusing into isolated, highly aligned multinucleated myotubes. **(A)** Phase-contrast image of myotube micropattern. **(B)** Muscle-specific staining for nicotinic acetylcholine receptors (AChR) using Alexa Fluor[®] 488-conjugated α -bungarotoxin. Note that clusters of AChRs formed spontaneously. **(C)** Nuclear counterstaining with DAPI. **(D)** Actin cytoskeleton stained with rhodamine-conjugated phalloidin.

2. Microfluidic Delivery of Soluble Factors to Muscle Cells

We have also developed a long-term (>2 weeks) microfluidic cell culture system that was designed to serve as an in vitro model for studying muscle cell differentiation and for characterization of extracellular molecules and mechanisms involved in the postsynaptic differentiation. The microfluidic cell culture device consists of a main fluidic channel formed by three converging inlet channels for focal delivery of relevant neurotransmitters to the target cells. The target cells—myoblasts—are micropatterned

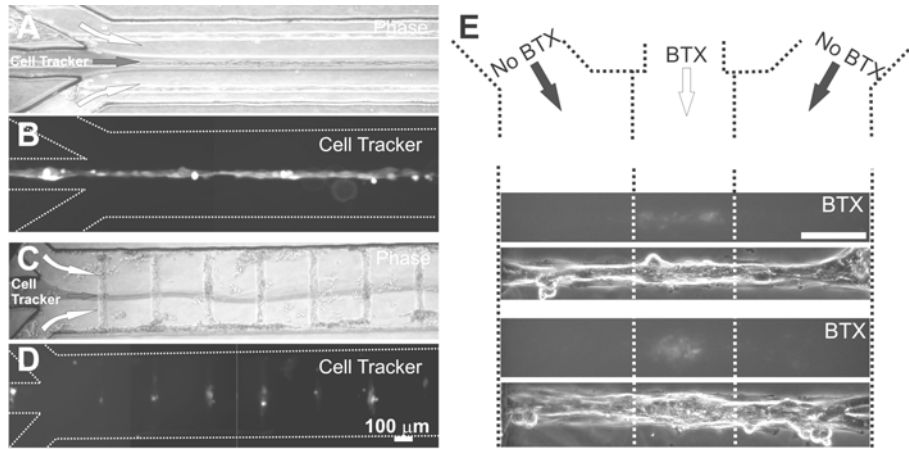


FIGURE 8. Long-term microfluidic muscle cell cultures. Shown are C2C12 cultures inside microchannels. Cells grew normally and formed myotubes within the microfluidic environment if constantly perfused with medium at a slow rate. Myotubes on the micropatterned surfaces aligned according to the geometry of the adhesive tracks. (A–D) Labeling with cell-permeable dyes: phase-contrast (A, C) images show muscle cells exposed to focused flow of a stream that contained fluorescent CellTracker™ and a food dye (Allura Red, for visualizing the stream with bright field illumination). Corresponding fluorescence images (B, D) show that only the part of the muscle cells exposed to CellTracker is actually labeled. (E) Membrane protein labeling with heterogeneous streams: Focal exposure of myotubes to Alexa Fluor® 488-conjugated α -bungarotoxin specifically labeled membrane receptor AChRs at selected positions. This microfluidic cell culture method has great potential for studying the effects of extracellular factors on muscle cell differentiation, such as the formation of the postsynaptic apparatus. Scale bars are 200 μ m.

on the bottom of the main channel. The formation of aligned isolated myotubes in the microfluidic culture is in agreement with traditional, random (non-microfluidic) cultures in terms of muscle cell-specific differentiation markers and the timing of fusion. This microfluidic system provides accurate control of the perfusion rates and of the chemical environment surrounding the cells, and allows us to locally present and precisely characterize the biomolecules in a physiologically relevant manner. As shown in Figure 8, by flowing fluorescent markers using heterogeneous laminar streams, it is possible to label cytoplasmic compartments (with CellTracker™, see Fig. 8A–D) and membrane proteins (such as acetylcholine receptors, labeled with fluorescently conjugated bungarotoxin, see Fig. 8E) with subcellular resolution.

3. Micropatterns of Cardiac Myocytes

Cardiac muscle fibers consist of organized cardiomyocytes with intracellular contractile myofibrils oriented parallel to the long axis of each cell and junctional complexes between abutting cells concentrated at the ends of each cardiomyocyte (but, unlike the skeletal muscle cells reviewed above, cardiomyocytes are not fused, thus do not form myotubes). The highly oriented cytoarchitecture is critical for the proper electromechanical coupling of cardiomyocytes to stimulate the transmission of directed contraction over long distances. Micropatterned cardiomyocyte cultures attempt to recreate this architecture in vitro, and hence may reproduce more faithfully the true physiological conditions of heart muscle and may be also useful for cell-based sensors and tissue engineering applications. Patterning heart cells in culture to create “cable-like” strands was first performed, without microfabrication techniques, by Lieberman and coworkers, who grew dissociated cells in grooves cut in agar^{217,218} or used nylon filaments as substrates.²¹⁹

Rohr et al.²²⁰ found that neonatal rat heart cells prefer to attach to glass over photoresist, so they used photoresist as the non-adherent material. In channels with width smaller than 100 μm , cells were aligned longitudinally and formed cross-striations as in vivo. Electrophysiological recording of these cells displayed a normal action potential and upstroke velocity. With micropatterned cells, it was also possible to assess the influence of cell geometry and organization on impulse propagation. The authors monitored the transmembrane voltage on multiple cells with voltage-sensitive dyes and observed the decrease in conduction velocity of an impulse propagating along a narrow cell strand as it entered a region of abrupt expansion. In contrast with the elongated and aligned cells forming the narrow strands, the cells forming the expansions were aligned at random and presented 2.5 times as many cell-to-cell appositions per unit length. If the decrease in conduction velocity resulted entirely from this increased number of cell-to-cell boundaries per unit length, the mean activation delay introduced by each boundary could be estimated to be 70 μs . Using this photoresist-based cell micropatterning method, the electrical coupling of fibroblasts and endothelial cells to myocytes in culture could be demonstrated.^{221,222}

Using the same techniques, Thomas et al.²²³ also morphologically and electrophysiologically characterized synthetic strands of mouse ventricular myocytes. Combined with immunocytochemistry staining of connexin, *N*-cadherins, and myosin to assess cell/cell connection and myofibril arrangement, they found that the myocyte strands resembled large mammal hearts in gap junction distribution and in conduction velocity. Using genetically engineered myocytes from Connexin43 (Cx43) *+/+* (wild type) and Cx43 *+/-* (heterozygote) mice, these researchers analyzed the influence of connexin reduction on cell morphology and electrical properties of the synthetic strands.²²⁴ They found that heterozygote-null mutation of Cx43

produced a complex electrical phenotype in synthetic strands with changes in both ion channel function and cell-to-cell coupling.

Microstamping has also been used to pattern cardiomyocytes. McDevitt et al.²²⁵ microstamped laminin lines (5–50 μm wide) on glass and on a biodegradable polymer (Fig. 3I). On both substrates, patterned cardiomyocytes displayed a striking bipolar localization of *N*-cadherin and connexin43 that resembled the intercalated disks found in vivo. By 48 hours after formation of intercalated disks within each lane, entire lanes of cardiomyocytes contracted in synchrony. When cells were seen bridging across narrow gaps (10 μm), different lanes beat in synchrony.²²⁵

Calcium-induced calcium release (CICR) is a critical mechanism for cardiomyocyte contraction. Kaji et al.²²⁶ patterned chick embryonic cardiac myocytes on fibronectin patterns microstamped on an octadecyl trichlorosilane SAM on glass. Myocytes aligned on fibronectin patterns as narrow as 5 μm . Calcium (fluorescence) imaging revealed that a calcium transient for each myocyte occurred simultaneously over the line pattern., consistent with CICR mechanism. Locally propagated planar and spiral calcium waves were also observed.

Gopalan et al.²²⁷ used micropatterned ventricular myocytes on deformable PDMS membranes to study anisotropic stretch-induced regulation of sarcomere organization, hypertrophy, and cell-to-cell junctions. Confluent, elongated, aligned myocytes were produced by varying the micropattern line width and collagen density. An elliptical cell stretcher applied 2:1 anisotropic strain statically to the elastic substrate, with the axis of greatest stretch (10%) either parallel or transverse to the myofibrils. They found that transverse rather than longitudinal stretch could significantly alter the expression of atrial natriuretic factor, connexin-43, or *N*-cadherin in myofibrils.

The cardiomyocytes patterns mentioned above are all 2-D patterns that allow forming monolayer strands of myofibers and allowing identifying each individual cell. Attempting to mimic the 3-D structure of in vivo cardium, Desai and colleagues²²⁸ microfabricated textured PDMS membranes consisting of grooves and posts using photolithography and microfabrication techniques. Cardiac myocytes plated on these membranes displayed stronger attachment and increased myofibril height compared to conventional culture substrates. On the vertical face of the microposts, cells terminated in a sarcomeric striation, whereas on nontextured surfaces they ended in long nonstriated cables. The focal adhesion protein vinculin was found to decrease in expression on combination surfaces, compared to nontextured substrata.²²⁹

4. Using Electrophysiology of Cardiomyocytes as Cell-Based Sensors

Because cardiomyocytes are also excitable cells, their electrical activity can be used as cell-based sensors. Planar MEAs have been used to stimulate and monitor physical

beating of cultured cardiomyocytes.²³⁰ Denyer et al.²³¹ studied the suitability of cardiac myocytes cultured over MEAs for a pharmacological bioassay. They could reliably record potentials with a mean amplitude of 16.9 μV and reversibly blocked the potential with micromolar concentrations of the sodium channel blocker lidocaine. Less common potentials with amplitudes of up to 3.5 mV were also recorded.

DeBusschere and Kovacs²⁰³ first developed a hand-held device capable of recording from cardiomyocytes outside of the laboratory. The device was an integrated silicon-PDMS cell cartridge containing a glass cover, a PDMS part forming two sealed cell chambers with independent fluidic channels, and a CMOS silicon chip that incorporated a digital interface, temperature control system, microelectrode electrophysiology sensors, and analog signal buffering. A portable, microcontroller-based electronics system capable of monitoring the action potential (AP) activity within the cell cartridges was also developed. As expected, the AP activities of murine atrial myocyte HL-1 cell line in the two chambers differentially responded to the flow of a control medium versus the flow of medium containing the calcium channel blocker nifedipine.

Aravenis et al.²³² used mouse cardiomyocytes in a differential genetically engineered cell-based biosensor (GECBB). The principle of the GECBB is to assay for a biological agent's ability to differentially activate two populations of cells—wild-type cells and “knockout” cells genetically engineered to lack a specific receptor; thus, the sensor can report both the baseline response of the wild-type cells and the knockout cells, which can then be used to infer the signaling pathway affected by the agent. To make a GECBB sensitive to agents that activate the beta 1-adrenergic receptor, cardiomyocytes from beta 1-AR knockout were used. The cellular signal used in the GECBB was the spontaneous beat rate of the two-cardiomyocyte syncytia as measured with microelectrode arrays. The GECBB was able to detect the beta-AR agonist isoproterenol (ISO) at a concentration of 10 μM .

V.E. Endothelial Cell Biology on a Chip

The endothelium is a single-cell layer lining the blood vessels and effectively constitutes the interface between blood and tissue. It acts as a selective permeability barrier, regulates coagulation, and contributes to the behavior of cells both in the circulation and in the vessel wall. Endothelial cells also produce cytokines and cell growth factors and promote wound healing. In addition, endothelial cells are also critically involved in the process of angiogenesis. Using cultures of rat thoracic aorta endothelial cells grown on thermoresponsive dishes, Soejima et al.²³³ demonstrated that grafted endothelial cells in culture displayed angiogenesis effects. A confluent layer of endothelial cells was detached as an intact sheet by a low-temperature treatment. Cell sheets were then grafted to 3 \times 3 cm full-thickness skin defects on the

backs of rats, in combination with either free skin grafts or artificial dermis grafts. Histological examinations showed that, with each of the grafting procedures, the number of vessels in a unit area (10^{-4} mm²) was significantly larger in the group with transplantation of cultured endothelial cells.²³³

Micro-controlling the positioning and spreading of endothelial cells facilitated the understanding of the control mechanism of cell growth by individual factors. Folkman and Moscona²³⁴ found in 1978 that cell spreading was tightly coupled to DNA synthesis and growth in nontransformed cells. This was demonstrated by varying tissue culture plastic adhesivity with different concentrations of poly(2-hydroxyethyl methacrylate). The use of cell culture surfaces such as SAMs with tunable surface physicochemical properties allows for inspecting the components of the complex interactions between cells and the ECM: surface charge, surface hydrophobicity, and other short- and long-range forces can be individually controlled and correlated with cellular functions.²³⁵ A range of techniques have been used to micropattern endothelial cells.²³⁶⁻²⁴³

Chen et al.²⁴⁴ found that cell spreading acted as a regulator of proliferation or death in human and bovine capillary endothelial (CE) cells by tightly controlling cell spreading with adhesive microislands of fibronectin; fibronectin was adsorbed on a methyl-terminated alkanethiol SAM, whereas the nonadhesive background consisted of a hexaethylene-glycol-terminated alkanethiol SAM (HEG-SAM) that resisted protein adsorption and cell attachment. Cells that were free to spread over large microislands displayed growth, as expected, but the cells that were constrained to limit their spreading to a small island displayed apoptosis. When cell spreading was varied while maintaining the total cell/matrix contact area constant by changing the spacing between multiple focal adhesion-sized (3 or 5 μ m diameter) islands, it was found that cell shape rather than total ECM contact area governed growth or death of individual cells.²⁴⁴ Huang et al.²⁴⁵ probed the molecular basis of shape-dependent growth control in CE cells using the same culture system. They showed that attached CE cells that were prevented from spreading failed to increase cyclin D1 levels or downregulate the cell cycle inhibitor p27Kip1 and hence were arrested in late G1 before pRb hyperphosphorylation. Disrupting the actin network or actomyosin interactions induced a similar block in cell cycle progression.

Control of cellular growth by cell/cell interactions has also been studied using carefully designed micropatterns. In homogenous (randomly seeded) cultures, increasing the density of endothelial or smooth muscle cells results in increased cell/cell contact and decreased cell spreading, leading to decreased proliferation. However, in these cultures it is not possible to distinguish between effects on proliferation caused by cell/cell contacts, paracrine signaling through soluble factors, and cell spreading. With cells cultured on square islands created by HEG-SAM microstamping, Nelson and Chen²⁴⁶ varied the number of cell/cell interactions independently of the extent of cell spreading (e.g., single cells on 625- μ m² islands have equal spreading but fewer

contacts than four cells on 2500- μm^2 islands) and vice versa. In agreement with their previous findings, they found that proliferation increased significantly with increasing cell spreading in isolated islands; it was interesting to note that at each degree of cell spreading, increasing cell/cell contact resulted in an additional statically significant increase in proliferation. To truly isolate the effects of cell spreading and cell/cell contact, they plated cells on bowtie-shaped fibronectin patterns surrounded by a 10- μm -thick layer of nonadhesive agarose (the fibronectin-coated surface was PDMS, and the space between the PDMS bowties was filled with agarose by microfluidic patterning, as described above¹⁸). The proliferation rate nearly doubled for cells grown in pairs (each cell spread in one half, 750 μm^2 per half) compared to single cells (one cell in one half, the other half empty). Intercellular adhesion molecules were found to localize to cell/cell contacts within 4 hours. However, in the absence of physical contact—that is, cells on substrates where the bowtie shaped pattern was bisected with a strip of nonadhesive agarose, leaving 2- and 5- μm -sized gaps between neighboring cells—the proliferation rates of cells grown in these separated pairs dropped to the levels of single cells, confirming that direct contact between cells and not diffusible signaling is responsible for the cell-pairing-induced increase in proliferation (Fig. 9). Pharmacological blocking of the PI₃K signaling pathway

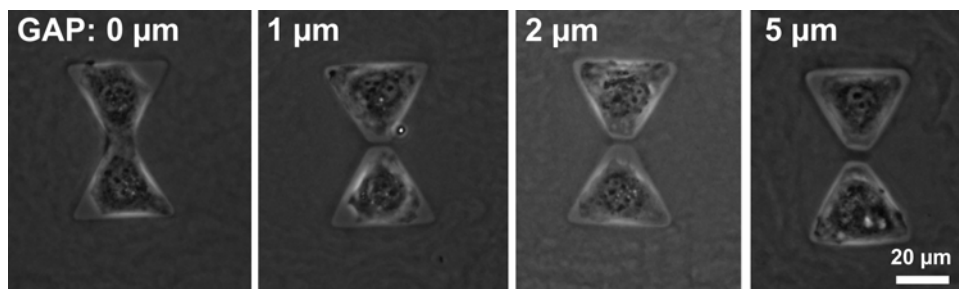


FIGURE 9. Effects of direct contact, paracrine signaling, and cell spreading on cell proliferation. Shown are phase contrast image of pairs of bovine pulmonary artery endothelial cells grown in bowtie patterns separated by 0, 1, 2, and 5 μm gaps. The 1–5 μm gaps were sufficiently narrow to allow proteins secreted by one cell in a pair to diffuse across to the other cell, based on a simple diffusion model. The authors found that, when cell spreading was kept constant, pairs of contacting endothelial cells (one cell in each half of the no-gap bowtie) proliferated more than single cells (single cells attach and spread primarily in half of the bowtie-shaped well with the other half empty). However, the proliferation rates of cells grown in these small gap-separated pairs dropped to the levels of single cells, indicating that direct contact between cells and not diffusible signaling was responsible for the increase in proliferation by cell/cell interactions. (Contributed by Chen and Nelson.²⁴⁶)

completely inhibited the increase in proliferation of pairs over single cell controls. In summary, introducing cell/cell contact positively regulates proliferation, and past studies of “contact inhibition” of growth of cells cultured in monolayers may be due to the contact-mediated proliferation being masked by changes in cell spreading.

The formation of organized multicellular assemblies of endothelial cells (ECs) into neovascular structures depends on cell/cell and cell/substrate interactions. Micropatterned substrates have been used to promote the differentiation of ECs by providing geometric control over neovascularization. Matsuda and Chung²⁴⁷ prepared glass substrates containing micrometer-scale grooves and holes using UV excimer laser ablation. ECs were observed to align along the 10- μm groove, resulting in very narrow tube-like tissue formation, whereas in a hole ECs tended to form a multilayered spherical aggregate; a single cell resided in a 10- μm^2 hole. Dike et al.²⁴⁸ fabricated 10- μm -wide lines of fibronectin by microstamping of alkanethiol SAMs; fibronectin was adsorbed on the stamped methyl-terminated alkanethiol SAM, whereas a HEG-SAM background resisted protein adsorption and cell spreading outside of the fibronectin lines. The ECs formed extensive cell/cell contacts and spread to approximately 1000 μm^2 . Within 72 hours, cells shut off both growth and apoptosis programs and underwent differentiation, resulting in the formation of capillary tube-like structures containing a central lumen (a common observation in EC cultures—in traditional, randomly seeded cultures the tube-like structures are randomly oriented, thus the lumens are very short). Accumulation of extracellular matrix tendrils containing fibronectin and laminin beneath cells and reorganization of platelet endothelial cell adhesion molecule-positive cell/cell junctions along the lengths of the tubes preceded the formation of these structures. Cells cultured on wider (30- μm) lines also formed cell/cell contacts and aligned their actin cytoskeleton, but these cells spread to larger areas (2200 μm^2), proliferated, and did not form tubes.²⁴⁸ Morphological patterning was also shown to affect the direction of lamellipodia extension²⁴⁹ and the migration of endothelial cells on micropatterned collagen strips.²⁵⁰ It may ultimately be possible to promote and control endothelial cell adhesion, growth, migration, and differentiation on the surface of micropatterned implanted materials to promote angiogenesis and wound healing.

V.F. Liver Cell Biology on a Chip

The liver is responsible for hundreds of biochemical processes vital to the organism, including detoxification, synthesis and secretion of plasma proteins, blood sugar regulation by gluconeogenesis, glycogen synthesis and secretion, lipid synthesis, urea synthesis, and bile synthesis and secretion. Primary cultures of mature hepatocytes retain many liver-specific functions (e.g., synthetic functions such as albumin expression, metabolic liver functions such as urea synthesis, and detoxification functions

such as cytochrome p450 activity) and respond to various hormones like cells *in vivo*. Substrates suitable for hepatocyte attachment include collagen, fibronectin, and poly *n*-vinylbenzyl-*D*-lactonamied (PVLA) (a lactose-derivative-modified polystyrene that specifically allows hepatocytes to adhere). The collagen “gel sandwich” configuration is a popular method for maintaining long-term hepatocyte functions.²⁵¹⁻²⁵⁹ Nonetheless, the successful development of cell-based artificial liver devices requires long-term, stable hepatocytic function in a perfusable environment and efficient transport of nutrients and waste within the device.

Several groups have created micropatterned hepatocytes by patterning collagen on various types of backgrounds; hepatocytes adhere to collagen with high selectivity. As expected, hepatocyte morphology is influenced by the shape of the adhesive collagen patterns: hepatocytes on narrow collagen strips display elongated shapes.^{18,37,260,261}

Singhvi et al.²⁶² cultured hepatocytes on micropatterns of laminin absorbed onto microstamped SAM patterns (laminin on alkanethiol SAMs, with a nonadhesive HEG-SAM) and found that limiting the degree of cell extension by decreasing the size of the adhesive islands resulted in a progressive reduction of growth and increase of albumin secretion. Hepatocytes cultured on unpatterned substrata rapidly lost the ability to secrete high levels of albumin, while hepatocytes maintained near-normal levels of albumin secretion for at least 3 days when cultured on the smallest adhesive islands that fully restrict cell extension. In general, albumin secretion rates decreased as the size of the adhesive island was increased, and growth was promoted. This result was an early indication that micropatterning cell shape can be used to switch the cells between a state of growth and of differentiation.

Micropatterned cocultures allow for probing the complex interplay between two or more cell types as they form a functional model tissue or organ. Toner's group^{18,38,39} pioneered the use of microfabrication techniques to coculture two cell types, in particular hepatocytes and fibroblasts. To ensure the differential attachment of two cell types, the two cell types were seeded sequentially on collagen micropatterns (background of albumin), exploiting differences in adhesivity of either cell type when the cells are seeded in serum-free medium (cells “respect” the adhesive/nonadhesive protein micropattern) versus cells seeded in serum-containing medium (the cells then attach both to collagen and to albumin, but the collagen is already occupied by the first cell type).

In both the developing and the adult liver, cell/cell interactions are imperative for coordinated organ function. Hence, cocultivation of hepatocytes with mesenchymal cells is widely used to stabilize the liver-specific function of isolated cells. Different approaches have been developed to produce co cultures of controlled ratio and position of hepatocytes and fibroblasts. Spheroids of fibroblasts and hepatocytes can be released from surfaces of the thermoresponsive polymer poly *N*-isopropyl acrylamide (PNIPAAm),^{263,264} but in spheroids the hepatocytes and fibroblasts

contact each other at random positions and ratios. To understand the stabilization effects of “heterotypic” cell interactions in liver cell cocultures (i.e., hepatocyte/fibroblast interactions), Bhatia et al.²⁶⁵ cultured cells on collagen micropatterns with the same total cell adhesion areas but varying heterotypic interface as a result of varying adhesive island size and center-to-center spacing. Increasing heterotypic interaction between fibroblasts and hepatocytes (i.e., by breaking down large islands into smaller islands of the same total sum area) caused an increase in levels of liver-specific functions (only albumin secretion and urea synthesis were probed). Intracellular albumin in hepatocytes in the vicinity of fibroblasts was increased as compared to hepatocytes far from the heterotypic interface. Further experiments with conditioned media and agitation suggested that heterotypic cell contact was necessary for induction of these functions. To probe the effect of “homotypic” fibroblast interactions (i.e., fibroblast/fibroblast interactions) on hepatic functions, the authors generated cocultures consisting of hepatocyte islands of fixed diameter surrounded by fibroblasts with progressive reduction in island spacing and total patterned surface area; therefore, the homotypic hepatocyte interactions and the heterotypic interface were held constant, and the number of fibroblasts was isolated as an independent variable. Increasing fibroblast number in both random and patterned cocultures greatly enhanced synthetic (albumin) and metabolic (urea) markers of liver-specific function in a dose-dependent manner.³⁹

V.G. Bone Cell Biology on a Chip

Motivated by promoting osteointegration of orthopedic and dental implants, Brunettes’s group²⁶⁶⁻²⁶⁸ investigated the effects of surface topography on the mineralization of implanted micromachined surfaces *in vivo* and *in vitro*. Different surface topographies were achieved by creating titanium-coated epoxy replicas of micromachined silicon masters. *In vitro*, osteoblasts from rat fetal calvaria preferred a grooved surface over a smooth one. Cell shape and cytoskeleton were strikingly influenced as early as 20 minutes after cell attachment, when the cytoskeleton began to align with the topographical features. Some grooved surfaces appeared to promote osteogenesis *in vitro* as assessed by the production of bone-like nodules, which aligned with the topography. When the grooved substrates were implanted subcutaneously in the parietal area of rats, after 6–8 weeks bone-like tissue was found adjacent to some micromachined surfaces but not on smooth surfaces. Mineralized matrix and collagen bundles were found contacting the titanium coating without any intervening material. The frequency of bonelike foci formation decreased as the depth of the grooves increased; in contrast, mineralization occurred more frequently as the depth of the pits increased. In addition, bone-like foci were oriented along the long axis of the grooves.²⁶⁶⁻²⁶⁸ These studies demonstrate that

the surface topography of an implant may promote bone tissue formation in vivo and in vitro.

Surface chemistry modification methods were also developed to control the attachment and functions of osteoblast cells. Lom et al.^{116,269} used patterns of aminosilane (*N*-(2-aminoethyl)-3-aminopropyl-trimethoxysilane [EDS]) and alkylsilane (dimethyldichlorosilane [DMS]) SAMs to spatially control the attachment of osteosarcoma cells; bone-derived cells required the presence of serum or vitronectin to organize in compliance with the lithographically defined surface chemistry.²⁷⁰ Cells were randomly distributed over the EDS/DMS surface at the time of plating but reorganized on the EDS regions within 30 minutes. Using a radial flow apparatus, they found that within 20 minutes, the strength of adhesion was significantly larger on EDS and clean surfaces than on DMS surfaces. Within 2 hours of cell incubation, there were no statistical differences among the strength of cell adhesion to EDS, DMS, and clean surfaces.²⁷¹ When cultures were extended for 15 and 25 days, the matrix synthesized by the cells was preferentially mineralized on the EDS surface. These results highlight the role of surface chemistry in organizing cells and forming mineralized tissue in vitro.²⁷²

To study adhesion, spreading, and focal contact formation of bone cells, Rezania et al.²⁷³ immobilized a 15-aminoacid peptide that contained an RGD (Arg-Gly Asp) sequence unique to bone sialoprotein. The peptide surfaces were fabricated by using a heterobifunctional crosslinker to link the peptide to amine-functionalized quartz surfaces. After 20 minutes of cell incubation, both the strength of cell adhesion and the mean area of cells contacting were significantly higher on RGD surfaces than on RGE (control) surfaces. Vinculin staining showed formation of small focal-contact patches on the periphery of bone cells incubated for 2 hours on the RGD surfaces, but few or no focal contacts on the RGE-grafted surfaces. Heterogeneous “mimetic peptide surfaces” (MPS) containing both the RGD (integrin-binding) and FHRRIKA (putative heparin-binding) peptides—unique to bone sialoprotein—in ratios of 75:25 (MPS II) or 50:50 (MPS III) proved to be more biologically relevant and specific for rat calvarial osteoblasts. MPS II and III surfaces enhanced cell spreading and long-term events such as mineralization of the extracellular matrix compared to homogeneous peptide surfaces and controls.²⁷⁴ Hasenbein et al.²⁷⁵ immobilized the cell-adhesive peptides RGDS and KRSR onto the aminosilane regions of microstamped aminosilane/alkylsilane patterns on borosilicate glass. In the absence of serum, after 4 hours both osteoblasts and fibroblasts adhered and formed clusters onto circles modified with the adhesive peptide RGDS, whereas only osteoblasts adhered and formed clusters onto the circles modified with KRSR, a peptide that selectively promotes adhesion of osteoblasts; adhesion of either osteoblasts or fibroblasts on surfaces patterned with the nonadhesive peptides RDGS and KSSR was random and low. These results provided evidence that patterning of select peptides can direct adhesion of specific cell lines exclusively to predetermined regions of a surface.

Bearinger et al.²⁷⁶ investigated the composition and properties of PEG IPN immobilized on metallic, polymeric, and ceramic materials. Protein adsorption experiments in 15% fetal bovine serum indicated that significant amounts of protein did not adsorb to the surface of the PEG IPN (~20 nm thick). Cell detachment experiments indicated that cells contacting copolymer-modified surfaces were removed by lower shear stresses than were cells contacting clean and amine-terminated, (*N*-(2-aminoethyl)-3-aminopropyl)-trimethoxysilane (EDS)-modified surfaces. Micropatterns of adhesive EDS and nonadhesive PEG IPN were used to control the projected area and shape of individual bone cells. The multidomain patterns consisted of over 3800 adhesive islands of circles, ellipses, squares, and rectangles ranging in projected area from 75 μm^2 to 10,000 μm^2 separated by 75 μm . Cells assumed the size and shape of the adhesive EDS region. With proper cell density, only one cell settled into one island. Actin staining showed that stress fibers organized as mandated by the shape (perimeter) of the adhesive region.²⁷⁷

PEG IPNs are naturally designed to resist materials fouling caused by nonspecific protein adsorption and indiscriminate cell or bacterial adhesion, but they can also be rendered cell-adhesive when the PEG IPN is modified with certain bioactive peptides. Rat calvarial osteoblasts attached to Arg-Gly Asp (RGD)-modified PEG IPNs at levels significantly greater than they did to clean quartz or to the control Arg-Gly Glu (RGE)-modified PEG IPNs (with or without serum in the medium). Cells maintained in media containing 15% fetal bovine serum (FBS) proliferated, exhibited nodule formation, and generated sheets of mineralized extracellular matrix (ECM) upon addition of β -glycerophosphate to the media.²⁷⁸ RGD-modified PEG IPNs on titanium supported osteoblast attachment, spreading, and significant mineralization.²⁷⁹

Stile and Healy^{280,281} characterized thermo-responsive peptide-modified hydrogels consisting of *N*-isopropylacrylamide (NIPAAm) and acrylic acid (AAc) as model scaffolds for studying cell/material interactions in 3-D. The AAc groups were functionalized with peptides containing the -RGD- or the -FHRRIKA- sequences explained above. The peptide-modified hydrogels were pliable at 22 °C and could be injected through a small-diameter aperture. At physiological temperature, the hydrogel increased rigidity. Rat calvarial osteoblasts cultured inside the peptide-modified hydrogels spread more and demonstrated significantly greater proliferation than within control hydrogels and were viable for at least 21 days in vitro. These peptide-modified P(NIPAAm-co-AAc) hydrogels could potentially be used as injectable scaffolds for tissue engineering applications.

V.H. Blood Cell Biology on a Chip

Microfabricated devices have been developed to measure human red blood cell deformability using a single micropore (diameters down to 1 μm) on a thin (0.4 μm thick)

Si_3N_4 film,²⁸² using 2.5–4- μm -wide microchannels on a silicon wafer^{283,284} or PDMS channels.^{285–287} Bitensky's group^{285,286} used an *in vitro* model of the blood microcirculatory system consisting of a network of PDMS microchannels patterned after the dimensions and architecture of the mammalian microcirculation. The device was cast in PDMS, and the channels were rendered hydrophilic to facilitate flow by immobilizing a PEG silane. The prototype contained 15 network units arranged in parallel and served by a distribution array upstream and an exit array downstream. Each network unit consisted of 34 microchannels of widths ranging from 6 to 63 μm and a uniform depth of 5.4 μm . Flow of red and white blood cells through the network was readily visualized. Sequences of high-quality images were used to calculate hematocrits and rates of red cell movement in the microchannels. Recently, Chiu and coworkers²⁸⁷ used a similar model to probe the obstruction of capillaries by malaria-infected red blood cells; unlike uninfected cells that can deform readily, the schizont and late-trophozoite forms of infected cells were not able to deform through a 4- μm constriction.

Microfabrication technology has also been used for studies of cell migration and chemotaxis of leukocytes. Tan et al.^{288,289} built arrays of physical obstructions on transparent (polyimide) materials for controlling cell motility on glass surfaces. Arrays of pillars and holes with 2 μm width, 4 μm height (or depth) separated by 10 μm were patterned using photolithography. Neutrophils attached and spread on the smooth glass surface and surfaces with pillars. In contrast, cells were rounded and did not adhere to either smooth polyimide film or films with holes. The migration of neutrophils was much faster on holes than on the polyimide surface but significantly slower on pillars than on glass. Such microstructured surfaces might be an effective tool for influencing cell migration in the design of biomaterials for tissue engineering.

Using microfluidically generated spatially and temporally steady gradients of chemotactic factors, Jeon et al.²⁹⁰ studied chemotaxis of human neutrophils in linear and complex gradients of interleukin-8 (IL-8). Different shapes of gradients were generated by controlled diffusive mixing of species in laminar-flow solutions inside a network of microchannels (reported previously²²). The cells exhibited strong directional migration toward increasing concentrations of IL-8 in linear gradients. Neutrophil migration halted abruptly (no overshoot) when cells encountered a sudden drop in the chemoattractant concentration to zero ("cliff" gradient). Unexpectedly, when neutrophils were challenged with a gradual increase and decrease in chemoattractant ("hill" gradient), the cells traversed the crest of maximum concentration and migrated farther ("overshoot") before reversing direction.

VI. To Be Continued ...

The literature of microfabricated cell-based devices and cell cultures is growing by the day. Examples abound of many biological questions being addressed by micro-

technology across many fields of biology not reviewed above. For example, Pins et al.⁵ made microtextured layers of collagen or gelatin (replicated from a PDMS mold that was in turn replicated from a laser-micromachined epoxy mold) to simulate the basal lamina of the skin; keratinocytes formed a differentiated and stratified epidermis that conformed to the surface of the membrane, and stratification in the deeper channels was enhanced compared to the shallower channels or the flat inter-channel regions, suggesting that part of the skin growth and differentiation program is governed by surface topography. In 1987, Hoch et al.²⁹¹ used microfabrication methods to simulate plant infection by spores, which were shown to grow using topographical guidance cues. Wheeler and colleagues^{292,293} have been able to manipulate single mammalian embryos through a network of microfluidic channels to manipulate the extracellular environment. Suh et al.²⁹⁴ presented an elegantly simple microfluidic device that separates motile from non-motile sperm: the device features two inlets, one main channel, and two outlets; as sperm is introduced into one of the inlets (the other one is for buffer), only the motile sperm are able to swim into the buffer part of the laminar flow and are taken by one of the opposite outlets. A similar microfluidic assay has been reported to measure bacterial chemotaxis.²⁹⁵

Undoubtedly, the list will continue to grow. It is worth noting that, although many techniques can be used for various cell types, the specific applicability of any given method to a certain cell type of interest should be carefully reassessed for each specific cell type and cell culture conditions.

VI. CONCLUSIONS AND FUTURE DIRECTIONS

Microfabrication techniques offer the potential to modulate, on a cellular and subcellular level, the biochemical composition as well as the topography of the substrate, the type of cell neighboring each cell, and the medium surrounding each cell. In this review, we examined examples of the unique applications of microfabrication in addressing biological questions. Topographical contact guidance of various cell types, from fibroblasts to neurons, has been studied with microfabricated substrates. Controlled differentiation and organization of neovascular or muscle tissues have been achieved by surface micropatterning. Organized cocultures of hepatocytes and fibroblasts for artificial liver development have also been realized. In addition, the effects of cell shape and intercellular signaling pathways on cell proliferation, differentiation, and communication have been probed for various cell types. Microfluidic delivery of soluble factors has provided a precise means to regulate neuronal growth, synaptic development, and neutrophil chemotaxis. Microfabrication has also enabled precise measurements on live cells, such as mechanical forces during cell traction or the electrical activity of excitable cells.

Compared to traditional cell culture techniques, microfabrication techniques, in combination with surface chemistry methods and microfluidic devices, have the intrinsic ability to precisely control and separate the effects of many of the parameters that affect cellular and subcellular events and signaling pathways. However, most current *in vitro* studies using microfabrication techniques have been conducted in an artificial 2-D environment (2-D cell patterns and/or constant flow conditions) that still cannot reproduce the complex 3-D organization found *in vivo*. Therefore, as in any cell culture study, results must be interpreted with caution and, whenever possible, be validated later with *in situ* and *in vivo* studies. Overall, substantial research is needed to better recapitulate *in vivo* environments.

The majority of the work reviewed here focused on novel effects that could be observed with microtechnology but not otherwise—i.e., it exploited the “small-scale benefit” of using microtechnology. However, an added benefit of microtechnology is that microsystems are most often amenable to high-throughput studies—either because microdevices cost less to operate, produce, or buy, or simply because they are smaller and faster. To date, in cell biology applications this “high-throughput benefit” has been put to use much less than the “small-scale benefit,” yet it comes at no added cost. We envision, therefore, that “lab-on-a-chip” applications, in which hundreds or thousands of cells will be cultured, controlled, and monitored in parallel on a small area and/or volume, will take full advantage of the microtechnological investment.

ACKNOWLEDGMENTS

We thank Dr. Xavier Figueroa for comments on the manuscript.

REFERENCES

1. Freshney RI. Culture of animal cells: A Manual of Basic Technique. 4th ed. New York: Wiley-Liss, 2000.
2. Folch A, Mezzour S, During M, Hurtado O, Toner M, Mueller R. Stacks of micro-fabricated structures for cell culture and tissue engineering. *Biomed Microdev* 2000; 2(3):207–214.
3. Liu VA, Bhatia SN. Three-dimensional photopatterning of hydrogels containing living cells. *Biomed Microdev* 2002; 4(4):257–266.
4. Petronis S, Eckert KL, Gold J, Wintermantel E. Microstructuring ceramic scaffolds for hepatocyte cell culture. *J Mater Sci Mater Med* 2001; 12(6):523–528.
5. Pins GD, Toner M, Morgan JR. Microfabrication of an analog of the basal lamina: biocompatible membranes with complex topographies. *FASEB J* 2000; 14:593.

6. Madou MJ. Fundamentals of microfabrication. Boca Raton, FL: CRC, 1997.
7. Ristic L, editor. Sensor technology and devices. Boston, MA: Artech House, 1994.
8. Fluitman J. Microsystems technology: objectives. *Sensors Actuators A Phys* 1996; A56(1–2):151–66.
9. Kovacs GTA, Petersen K, Albin M. Silicon micromachining—sensors to systems. *Anal Chem* 1996; 68(13):407A–412A.
10. Kleinfeld D, Kahler KH, Hockberger PE. Controlled outgrowth of dissociated neurons on patterned substrates. *J Neurosci* 1988; 8(11):4098–120.
11. Kumar A, Whitesides GM. Features of gold having micrometer to centimeter dimensions can be formed through a combination of stamping with an elastomeric stamp and an alkanethiol ink followed by chemical etching. *Appl Phys Lett* 1993; 63(14):2002.
12. Xia YN, Whitesides GM. Soft lithography. *Angew. Chem Int Edit Engl* 1998; 37(5):551.
13. Mrksich M, Whitesides GM. Patterning self-assembled monolayers using microcontact printing - a new technology for biosensors. *Trends Biotech* 1995; 13(6):228.
14. Qin D, Xia YN, Rogers JA, Jackman RJ, Zhao XM, Whitesides GM. Microfabrication, microstructures and microsystems. *Top Curr Chem* 1998; 194:1.
15. Whitesides GM, Ostuni E, Takayama S, Jiang XY, Ingber DE. Soft lithography in biology and biochemistry. *Annu Rev Biomed Eng* 2001; 3:335–73.
16. Kim E, Xia YN, Whitesides GM. Polymer microstructures formed by molding in capillaries. *Nature* 1995; 376(6541):581.
17. Delamarche E, Bernard A, Schmid H, Michel B, Biebuyck H. Patterned delivery of immunoglobulins to surfaces using microfluidic networks. *Science* 1997; 276(5313):779–81.
18. Folch A, Toner M. Cellular micropatterns on biocompatible materials. *Biotechnol. Prog.* 1998; 14(3):388–92.
19. Folch A, Ayon A, Hurtado O, Schmidt MA, Toner M. Molding of deep polydimethylsiloxane microstructures for microfluidics and biological applications. *J Biomech. Eng.* 1999; 121(1):28.
20. Chiu DT, Jeon NL, Huang S, Kane RS, Wargo CJ, Choi IS, et al. Patterned deposition of cells and proteins onto surfaces by using three-dimensional microfluidic systems. *Proc Natl Acad Sci U S A* 2000; 97(6):2408–2413.
21. Kenis PJA, Ismagilov RF, Whitesides GM. Microfabrication inside capillaries using multiphase laminar flow patterning. *Science* 1999; 285(5424):83.
22. Jeon NL, Dertinger SKW, Chiu DT, Choi IS, Stroock AD, Whitesides GM. Generation of solution and surface gradients using microfluidic systems. *Langmuir* 2000; 16(22):8311–8316.
23. Bernard A, Delamarche E, Schmid H, Michel B, Bosshard HR, Biebuyck H. Printing patterns of proteins. *Langmuir* 1998; 14(9):2225.
24. Branch DW, Corey JM, Weyhenmeyer JA, Brewer GJ, Wheeler BC. Microstamp patterns of biomolecules for high-resolution neuronal networks. *Med Biol Eng Comput* 1998; 36(1):135–41.
25. James CD, Davis RC, Kam L, Craighead HG, Isaacson M, Turner JN, et al. Patterned protein layers on solid substrates by thin stamp microcontact printing. *Langmuir* 1998; 14(4):741.

26. Tien J, Nelson CM, Chen CS. Fabrication of aligned microstructures with a single elastomeric stamp. *Proc Natl Acad Sci USA* 2002; 99(4):1758–62.
27. Folch A, Jo B-H, Beebe D, Toner M. Microfabricated elastomeric stencils for micropatterning cell cultures. *J Biomed Mater Res* 2000; 52(2):346–53.
28. Tourovskaia A, Barber T, Wickes BT, Hirdes D, Grin B, Castner DG, Healy KE, Folch A. Micropatterns of chemisorbed cell adhesion-repellent films using oxygen plasma etching and elastomeric stencils. *Langmuir* 2003; 19:4754–64.
29. Jackman RJ, Duffy DC, Cherniavskaya O, Whitesides GM. Using elastomeric membranes as dry resists and for dry lift-off. *Langmuir* 1999; 15(8):2973.
30. Ostuni E, Kane R, Chen CS, Ingber DE, Whitesides GM. Patterning mammalian cells using elastomeric membranes. *Langmuir* 2000; 16(20):7811–9.
31. Massia SP, Hubbell JA. Covalent surface immobilization of Arg-Gly-Asp- and Tyr-Ile-Gly-Ser-Arg- containing peptides to obtain well-defined cell-adhesive substrates. *Anal Biochem* 1990; 187(2):292–301.
32. Izzard CS, Lochner LR. Cell-to-substrate contacts in living fibroblasts: an interference reflexion study with an evaluation of the technique. *J Cell Sci* 1976; 21(1):129–59.
33. Wehland J, Osborn M, Weber K. Cell-to-substratum contacts in living cells: a direct correlation between interference-reflexion and indirect-immunofluorescence microscopy using antibodies against actin and alpha-actinin. *J Cell Sci* 1979; 37:257–73.
34. Grinnell F. Visualization of cell-substratum adhesion plaques by antibody exclusion. *Cell Biol Int Rep* 1980; 4(11):1031–6.
35. Ruoslahti E, Reed JC. Anchorage dependence, integrins, and apoptosis. *Cell* 1994; 77(4):477–8.
36. Folch A, Toner M. Microengineering of cellular interactions. *Annu Rev Biomed Eng* 2000; 2:227–256.
37. Bhatia SN, Toner M, Tompkins RG, Yarmush ML. Selective adhesion of hepatocytes on patterned surfaces. *Ann NY Acad Sci* 1994; 745:187–209.
38. Bhatia SN, Yarmush ML, Toner M. Controlling cell interactions by micropatterning in co-cultures: hepatocytes and 3T3 fibroblasts. *J Biomed Mater Res* 1997; 34(2):189–99.
39. Bhatia SN, Balis UJ, Yarmush ML, Toner M. Microfabrication of hepatocyte/fibroblast co-cultures: role of homotypic cell interactions. *Biotechnol Prog* 1998; 14(3):378–87.
40. Ulman A. An introduction to ultrathin organic films: from Langmuir-Blodgett to self-assembly. Boston, MA: Academic Press, 1991.
41. Joyce SA, Thomas RC, Houston JE, Michalske TA, Crooks RM. Mechanical relaxation of organic monolayer films measured by force microscopy. *Phys Rev Lett* 1992; 68(18):2790.
42. Salmeron M, Neubauer G, Folch A, Tomitori M, Ogletree DF, Sautet P. Viscoelastic and electrical-properties of self-assembled monolayers on Au(111) films. *Langmuir* 1993; 9(12):3600.
43. Bain CD, Whitesides GM. Molecular-level control over surface order in self-assembled monolayer films of thiols on gold. *Science* 1988; 240(4848):62.
44. Prime KL, Whitesides GM. Self-assembled organic monolayers: model systems for studying adsorption of proteins at surfaces. *Science* 1991; 252(5010):1164–7.
45. Drumheller PD, Hubbell JA. Surface immobilization of adhesion ligands for investiga-

- tions of cell-substrate interactions. In: Bronzino JD, editor. *The Biomedical Engineering Handbook*. Boca Raton, FL: CRC Press, 1995.
46. Massia SP, Hubbell JA. Covalently attached GRGD on polymer surfaces promotes biospecific adhesion of mammalian cells. *Ann NY Acad Sci* 1990; 589:261–70.
 47. Yousaf MN, Houseman BT, Mrksich M. Using electroactive substrates to pattern the attachment of two different cell populations. *Proc Natl Acad Sci USA* 2001; 98(11): 5992–6.
 48. Sigal GB, Bamdad C, Barberis A, Strominger J, Whitesides GM. A self-assembled monolayer for the binding and study of histidine-tagged proteins by surface plasmon resonance. *Anal Chem* 1996; 68(3):490–7.
 49. Knoll W, Liley M, Piscevic D, Spinke J, Tarlov MJ. Supramolecular architectures for the functionalization of solid surfaces. *Adv Biophys* 1997; 34:231–51.
 50. Holly FJ, Owen MJ. In: Mittal K, editor. *Physicochemical aspects of polymer surfaces*. New York: Plenum; 1981.
 51. Morra M, Ochiello E, Marola R, Garbassi F, Johnson D. *Colloid Interface Sci* 1990; 137:11.
 52. Gombotz WR, Wang GH, Horbett TA, Hoffman AS. Protein adsorption to poly(ethylene oxide) surfaces. *J Biomed Mater Res* 1991; 25(12):1547–62.
 53. Chaudhury MK, Whitesides GM. Direct measurement of interfacial interactions between semispherical lenses and flat sheets of poly(dimethylsiloxane) and their chemical derivatives. *Langmuir* 1991; 7(5):1013.
 54. Vargo TG, Gardella JA, Calvert JM, Chen MS. Adhesive electroless metallization of fluoropolymeric substrates. *Science* 1993; 262(5140):1711.
 55. Ferguson GS, Chaudhury MK, Biebuyck HA, Whitesides GM. Monolayers on disordered substrates - self-assembly of alkyltrichlorosilanes on surface-modified polyethylene and poly(dimethylsiloxane). *Macromolecules* 1993; 26(22):5870.
 56. Garbassi F, Morra M, Occhiello E. *Polymer Surfaces: From Physics to Technology*. England: Wiley, 1994.
 57. Mrksich M, Whitesides GM. Using self-assembled monolayers to understand the interactions of man-made surfaces with proteins and cells. *Annu Rev Biophys Biomol Struct* 1996; 25:55–78.
 58. Mrksich M. Tailored substrates for studies of attached cell culture. *Cell Mol Life Sci* 1998; 54(7):653–662.
 59. Takezawa T, Mori Y, Yoshizato K. Cell culture on a thermo-responsive polymer surface. *Biotechnology* 1990; 8(9):854–6.
 60. Ito Y, Chen GP, Guan YQ, Imanishi Y. Patterned immobilization of thermoresponsive polymer. *Langmuir* 1997; 13(10):2756.
 61. Chen G, Imanishi Y, Ito Y. Effect of protein and cell behavior on pattern-grafted thermoresponsive polymer. *J Biomed Mater Res* 1998; 42(1):38–44.
 62. Chen GP, Ito Y, Imanishi Y. Regulation of growth and adhesion of cultured cells by insulin conjugated with thermoresponsive polymers. *Biotechnol Bioeng* 1997; 53(3): 339.
 63. Ito Y, Chen GP, Imanishi Y. Artificial juxtacrine stimulation for tissue engineering. *J Biomater Sci Polym Ed* 1998; 9(8):879.
 64. Jiang X, Ferrigno R, Mrksich M, Whitesides GM. Electrochemical desorption of self-assembled monolayers noninvasively releases patterned cells from geometrical confinements. *J Am Chem Soc* 2003; 125(9):2366–7.

65. Chen GP, Ito YY. Gradient micropattern immobilization of EGF to investigate the effect of artificial juxtacrine stimulation. *Biomaterials* 2001; 22(18):2453–7.
66. Herbert CB, McLernon TL, Hypolite CL, Adams DN, Pikus L, Huang CC, et al. Micropatterning gradients and controlling surface densities of photoactivatable biomolecules on self-assembled monolayers of oligo(ethylene glycol) alkanethiolates. *Chem Biol* 1997; 4(10):731–7.
67. Dertinger SKW, Chiu DT, Jeon NL, Whitesides GM. Generation of gradients having complex shapes using microfluidic networks. *Anal Chem* 2001; 73(6):1240–6.
68. Dertinger SK, Jiang X, Li Z, Murthy VN, Whitesides GM. Gradients of substrate-bound laminin orient axonal specification of neurons. *Proc Natl Acad Sci USA* 2002; 99(20):12542–7.
69. Beebe DJ, Mensing GA, Walker GM. Physics and applications of microfluidics in biology. *Annu Rev Biomed Eng* 2002; 4:261–86.
70. White FM. *Fluid Mechanics*. New York: McGraw-Hill, 1979.
71. Kamholz AE, Weigl BH, Finlayson BA, Yager P. Quantitative analysis of molecular interaction in a microfluidic channel: the T-sensor. *Anal Chem* 1999; 71(23):5340–7.
72. Ismagilov RF, Stroock AD, Kenis PJA, Whitesides G, Stone HA. Experimental and theoretical scaling laws for transverse diffusive broadening in two-phase laminar flows in microchannels. *Appl Phys Lett* 2000; 76(17):2376–8.
73. Takayama S, McDonald JC, Ostuni E, Liang MN, Kenis PJA, Ismagilov RF, et al. Patterning cells and their environments using multiple laminar fluid flows in capillary networks. *Proc Natl Acad Sci USA* 1999; 96(10):5545.
74. Takayama S, Ostuni E, LeDuc P, Naruse K, Ingber DE, Whitesides GM. Laminar flows—subcellular positioning of small molecules. *Nature* 2001; 411(6841):1016.
75. Takayama S, Ostuni E, LeDuc P, Naruse K, Ingber DE, Whitesides GM. Selective chemical treatment of cellular microdomains using multiple laminar streams. *Chem Biol* 2003; 10(2):123–30.
76. Carter SB. Haptotactic islands: a method of confining single cells to study individual cell reactions and clone formation. *Exp Cell Res* 1967; 48(1):189–93.
77. Brunette DM. Fibroblasts on micromachined substrata orient hierarchically to grooves of different dimensions. *Exp Cell Res* 1986; 164(1):11–26.
78. Oakley C, Brunette DM. The sequence of alignment of microtubules, focal contacts and actin-filaments in fibroblasts spreading on smooth and grooved titanium substrata. *J Cell Sci* 1993; 106:343.
79. Oakley C, Brunette DM. Topographic compensation: guidance and directed locomotion of fibroblasts on grooved micromachined substrata in the absence of microtubules. *Cell Motil Cytoskeleton* 1995; 31(1):45–58.
80. Oakley C, Jaeger NA, Brunette DM. Sensitivity of fibroblasts and their cytoskeletons to substratum topographies: topographic guidance and topographic compensation by micromachined grooves of different dimensions. *Exp Cell Res* 1997; 234(2):413–24.
81. Wojciakstothard B, Curtis ASG, Monaghan W, McGrath M, Sommer I, Wilkinson CDW. Role of the cytoskeleton in the reaction of fibroblasts to multiple grooved substrata. *Cell Motility Cytoskel* 1995; 31(2):147.
82. Clark P. Cell behavior on micropatterned surfaces. *Biosens Bioelectron* 1994; 9(9–10):657–661.

83. Clark P, Connolly P, Curtis AS, Dow JA, Wilkinson CD. Topographical control of cell behaviour. I. Simple step cues. *Development* 1987; 99(3):439–48.
84. Clark P, Connolly P, Curtis AS, Dow JA, Wilkinson CD. Topographical control of cell behaviour: II. Multiple grooved substrata. *Development* 1990; 108(4):635–44.
85. Clark P, Connolly P, Curtis AS, Dow JA, Wilkinson CD. Cell guidance by ultrafine topography in vitro. *J Cell Sci* 1991; 99(Pt 1):73–7.
86. Clark P, Connolly P, Moores GR. Cell guidance by micropatterned adhesiveness in vitro. *J Cell Sci* 1992; 103:287–92.
87. Meyle J, Gultig K, Nisch W. Variation in contact guidance by human cells on a microstructured surface [published erratum appears in *J Biomed Mater Res* 1995 Jul; 29(7):905]. *J Biomed Mater Res* 1995; 29(1):81–8.
88. van Kooten TG, Whitesides JF, von Recum A. Influence of silicone (PDMS) surface texture on human skin fibroblast proliferation as determined by cell cycle analysis. *J Biomed Mater Res* 1998; 43(1):1–14.
89. Wojciak B, Crossan J, Curtis ASG, Wilkinson CDW. Grooved substrata facilitate in-vitro healing of completely divided flexor tendons. *J Mater Sci Mater Med* 1995; 6(5):266.
90. Britland S, Morgan H, WojciakStodart B, Riehle M, Curtis A, Wilkinson C. Synergistic and hierarchical adhesive and topographic guidance of BHK cells. *Exp Cell Res* 1996; 228(2):313.
91. Ireland GW, Dopping-Hepenstal P, Jordan P, O'Neill C. Effect of patterned surfaces of adhesive islands on the shape, cytoskeleton, adhesion and behaviour of Swiss mouse 3T3 fibroblasts. *J Cell Sci Suppl* 1987; 8:19–33.
92. Ireland GW, Dopping-Hepenstal PJ, Jordan PW, O'Neill CH. Limitation of substratum size alters cytoskeletal organization and behaviour of Swiss 3T3 fibroblasts. *Cell Biol Int Rep* 1989; 13(9):781–90.
93. O'Neill C, Jordan P, Riddle P, Ireland G. Narrow linear strips of adhesive substratum are powerful inducers of both growth and total focal contact area. *J Cell Sci* 1990; 95(Pt 4):577–86.
94. Chou L, Firth JD, Uitto VJ, Brunette DM. Substratum surface topography alters cell shape and regulates fibronectin mRNA level, mRNA stability, secretion and assembly in human fibroblasts. *J Cell Sci* 1995; 108(Pt 4):1563–73.
95. Harris AK, Wild P, Stopak D. Silicone rubber substrata: a new wrinkle in the study of cell locomotion. *Science* 1980; 208(4440):177–9.
96. Burton K, Park JH, Taylor DL. Keratocytes generate traction forces in two phases. *Mol Biol Cell* 1999; 10(11):3745–69.
97. Dembo M, Wang YL. Stresses at the cell-to-substrate interface during locomotion of fibroblasts. *Biophys J* 1999; 76(4):2307–16.
98. Munevar S, Wang Y, Dembo M. Traction force microscopy of migrating normal and H-ras transformed 3T3 fibroblasts. *Biophys J* 2001; 80(4):1744–57.
99. Lee J, Leonard M, Oliver T, Ishihara A, Jacobson K. Traction forces generated by locomoting keratocytes. *J Cell Biol* 1994; 127(6 Pt 2):1957–64.
100. Galbraith CG, Sheetz MP. A micromachined device provides a new bend on fibroblast traction forces. *Proc Natl Acad Sci USA* 1997; 94(17):9114–8.
101. Balaban NQ, Schwarz US, Riveline D, Goichberg P, Tzur G, Sabanay I, et al. Force and focal adhesion assembly: a close relationship studied using elastic micropatterned substrates. *Nat Cell Biol* 2001; 3(5):466–72.

102. Tan JL, Tien J, Pirone DM, Gray DS, Bhadriraju K, Chen CS. Cells lying on a bed of microneedles: an approach to isolate mechanical force. *Proc Natl Acad Sci USA* 2003; 100(4):1484–9.
103. Giaever I, Keese CR. Micromotion of mammalian-cells measured electrically. *Proc Natl Acad Sci USA* 1991; 88(17):7896–900.
104. Wegener J, Keese CR, Giaever I. Electric cell-substrate impedance sensing (ECIS) as a noninvasive means to monitor the kinetics of cell spreading to artificial surfaces. *Exp Cell Res* 2000; 259(1):158–66.
105. Hagedorn R, Fuhr G, Lichtwardt-zinke K, Richter E, Hornung J, Voigt A. Characterization of cell movement by impedance measurement on fibroblasts grown on perforated Si-membranes. *Biochim Biophys Acta Molec Cell Res* 1995; 1269(3):221–32.
106. Letourneau PC. Possible roles for cell-to-substratum adhesion in neuronal morphogenesis. *Dev Biol* 1975; 44(1):77–91.
107. Cooper A, Munden HR, Brown GL. The growth of mouse neuroblastoma cells in controlled orientations on thin films of silicon monoxide. *Exp Cell Res* 1976; 103(2): 435–9.
108. Hammarback JA, Palm SL, Furcht LT, Letourneau PC. Guidance of neurite outgrowth by pathways of substratum-adsorbed laminin. *J Neurosci Res* 1985; 13(1–2): 213–20.
109. Hammarback JA, McCarthy JB, Palm SL, Furcht LT, Letourneau PC. Growth cone guidance by substrate-bound laminin pathways is correlated with neuron-to-pathway adhesivity. *Dev Biol* 1988; 126(1):29–39.
110. Hammarback JA, Letourneau PC. Neurite extension across regions of low cell-substratum adhesivity: implications for the guidepost hypothesis of axonal pathfinding. *Dev Biol* 1986; 117(2):655–62.
111. Gundersen RW. Sensory neurite growth cone guidance by substrate adsorbed nerve growth factor. *J Neurosci Res* 1985; 13(1–2):199–212.
112. Gundersen RW. Response of sensory neurites and growth cones to patterned substrata of laminin and fibronectin in vitro. *Dev Biol* 1987; 121(2):423–31.
113. Stenger DA, Georger JH, Dulcey CS, Hickman JJ, Rudolph AS, Nielsen TB, et al. Coplanar molecular assemblies of aminoalkylsilane and perfluorinated alkylsilane—characterization and geometric definition of mammalian-cell adhesion and growth. *J Am Chem Soc* 1992; 114(22):8435.
114. Georger JH, Stenger DA, Rudolph AS, Hickman JJ, Dulcey CS, Fare TL. Coplanar patterns of self-assembled monolayers for selective cell-adhesion and outgrowth. *Thin Solid Films* 1992; 210(1–2):716.
115. Hickman JJ, Bhatia SK, Quong JN, Shoen P, Stenger DA, Pike CJ, et al. Rational pattern design for in-vitro cellular networks using surface photochemistry. *J Vac Sci Technol A* 1994; 12(3):607.
116. Lom B, Healy KE, Hockberger PE. A versatile technique for patterning biomolecules onto glass coverslips. *J Neurosci Methods* 1993; 50(3):385–97.
117. Corey JM, Wheeler BC, Brewer GJ. Micrometer resolution silane-based patterning of hippocampal neurons: critical variables in photoresist and laser ablation processes for substrate fabrication. *IEEE Trans Biomed Eng* 1996; 43(9):944–55.
118. Ruardij TG, Goedbloed MH, Rutten WL. Adhesion and patterning of cortical neurons on polyethylenimine- and fluorocarbon-coated surfaces. *IEEE Trans Biomed Eng* 2000; 47(12):1593–9.

119. Torimitsu K, Kawana A. Selective outgrowth of sensory nerve fibers on metal oxide pattern in culture. *Dev Brain Res* 1990; 51:128–131.
120. Dulcey CS, Georger JH, Jr., Krauthamer V, Stenger DA, Fare TL, Calvert JM. Deep UV photochemistry of chemisorbed monolayers: patterned coplanar molecular assemblies. *Science* 1991; 252(5005):551–4.
121. Matsuzawa M, Potember RS, Stenger DA, Krauthamer V. Containment and growth of neuroblastoma cells on chemically patterned substrates. *J Neurosci Methods* 1993; 50(2):253–60.
122. Matsuzawa M, Liesi P, Knoll W. Chemically modifying glass surfaces to study substratum-guided neurite outgrowth in culture. *J Neurosci Methods* 1996; 69(2):189–96.
123. Lee JS, Sugioka K, Toyoda K, Offenhausser A, Knoll W, Sasabe H. Micropatterning of cultured-cells on polystyrene surface by using an excimer-laser. *Appl Phys Lett* 1994; 65(4):400.
124. Corey JM, Wheeler BC, Brewer GJ. Compliance of hippocampal neurons to patterned substrate networks. *J Neurosci Res* 1991; 30(2):300–7.
125. Branch DW, Wheeler BC, Brewer GJ, Leckband DE. Long-term stability of grafted polyethylene glycol surfaces for use with microstamped substrates in neuronal cell culture. *Biomaterials* 2001; 22(10):1035–47.
126. Chang JC, Brewer GJ, Wheeler BC. A modified microstamping technique enhances polylysine transfer and neuronal cell patterning. *Biomaterials* 2003; 24(17):2863–70.
127. Lauer L, Klein C, Offenhausser A. Spot compliant neuronal networks by structure optimized micro-contact printing. *Biomaterials* 2001; 22(13):1925–32.
128. Degenaar P, Le Pioufle B, Griscom L, Tixier A, Akagi Y, Morita Y, et al. A method for micrometer resolution patterning of primary culture neurons for SPM analysis. *J Biochem (Tokyo)* 2001; 130(3):367–376.
129. Kam L, Shain W, Turner JN, Bizios R. Axonal outgrowth of hippocampal neurons on micro-scale networks of polylysine-conjugated laminin. *Biomaterials* 2001; 22(10):1049–54.
130. Lhoest JB, Detrait E, Dewez JL, van den Bosch de Aguilar P, Bertrand P. A new plasma-based method to promote cell adhesion on micrometric tracks on polystyrene substrates. *J Biomater Sci Polym Ed* 1996; 7(12):1039–54.
131. Detrait E, Lhoest JB, Knoops B, Bertrand P, van den Bosch de Aguilar P. Orientation of cell adhesion and growth on patterned heterogeneous polystyrene surface. *J Neurosci Methods* 1998; 84(1–2):193–204.
132. Ranieri JP, Bellamkonda R, Bekos EJ, Gardella JA, Jr., Mathieu HJ, Ruiz L, et al. Spatial control of neuronal cell attachment and differentiation on covalently patterned laminin oligopeptide substrates. *Int J Dev Neurosci* 1994; 12(8):725–35.
133. Ranieri JP, Bellamkonda R, Bekos EJ, Vargo TG, Gardella JA Jr, Aebischer P. Neuronal cell attachment to fluorinated ethylene propylene films with covalently immobilized laminin oligopeptides YIGSR and IKVAV. II. *J Biomed Mater Res* 1995; 29(6):779–85.
134. Vargo TG, Bekos EJ, Kim YS, Ranieri JP, Bellamkonda R, Aebischer P, et al. Synthesis and characterization of fluoropolymeric substrata with immobilized minimal peptide sequences for cell adhesion studies. I. *J Biomed Mater Res* 1995; 29(6):767–78.
135. Clemence JF, Ranieri JP, Aebischer P, Sigris H. Photoimmobilization of a bioactive

- laminin fragment and pattern-guided selective neuronal cell attachment. *Bioconjug Chem* 1995; 6(4):411–7.
136. Saneinejad S, Shoichet MS. Patterned glass surfaces direct cell adhesion and process outgrowth of primary neurons of the central nervous system. *J Biomed Mater Res* 1998; 42(1):13.
 137. Huber M, Heiduschka P, Kienle S, Pavlidis C, Mack J, Walk T, et al. Modification of glassy carbon surfaces with synthetic laminin-derived peptides for nerve cell attachment and neurite growth. *J Biomed Mater Res* 1998; 41(2):278–88.
 138. Matsuzawa M, Kobayashi K, Sugioka K, Knoll W. A biocompatible interface for the geometrical guidance of central neurons in vitro. *J Colloid Interface Sci* 1998; 202(2): 213.
 139. Yeung CK, Lauer L, Offenhausser A, Knoll W. Modulation of the growth and guidance of rat brain stem neurons using patterned extracellular matrix proteins. *Neurosci Lett* 2001; 301(2):147–50.
 140. Sukenik CN, Balachander N, Culp LA, Lewandowska K, Merritt K. Modulation of cell adhesion by modification of titanium surfaces with covalently attached self-assembled monolayers. *J Biomed Mater Res* 1990; 24(10):1307–23.
 141. Vargo TG, Thompson PM, Gerenser LJ, Valentini RF, Aebischer P, Hook DJ, et al. Monolayer chemical lithography and characterization of fluoropolymer films. *Langmuir* 1992; 8(1):130.
 142. Ranieri JP, Bellamkonda R, Jacob J, Vargo TG, Gardella JA, Aebischer P. Selective neuronal cell attachment to a covalently patterned monoamine on fluorinated ethylene propylene films. *J Biomed Mater Res* 1993; 27(7):917–25.
 143. Bekos EJ, Ranieri JP, Aebischer P, Gardella JA, Bright FV. Structural-changes of bovine serum-albumin upon adsorption to modified fluoropolymer substrates used for neural cell attachment studies. *Langmuir* 1995; 11(3):984.
 144. Makohliso SA, Giovangrandi L, Leonard D, Mathieu HJ, Ilegems M, Aebischer P. Application of Teflon-AF thin films for bio-patterning of neural cell adhesion. *Biosens Bioelectron* 1998; 13(11):1227–35.
 145. Patel N, Padera R, Sanders GHW, Cannizzaro SM, Davies MC, Langer R, et al. Spatially controlled cell engineering on biodegradable polymer surfaces. *FASEB J*. 1998; 12(14):1447–54.
 146. Stenger DA, Hickman JJ, Bateman KE, Ravenscroft MS, Ma W, Pancrazio JJ, et al. Microlithographic determination of axonal/dendritic polarity in cultured hippocampal neurons. *J Neurosci Methods* 1998; 82(2):167.
 147. Clark P, Britland S, Connolly P. Growth cone guidance and neuron morphology on micropatterned laminin surfaces. *J Cell Sci* 1993; 105(Pt 1):203–12.
 148. Aebischer P, Guenard V, Valentini RF. The morphology of regenerating peripheral nerves is modulated by the surface microgeometry of polymeric guidance channels. *Brain Res* 1990; 531(1–2):211–8.
 149. Nagata I, Kawana A, Nakatsuji N. Perpendicular contact guidance of CNS neuroblasts on artificial microstructures. *Development* 1993; 117(1):401–8.
 150. Rajnicek AM, Britland S, McCaig CD. Contact guidance of CNS neurites on grooved quartz: influence of groove dimensions, neuronal age and cell type. *J Cell Sci* 1997; 110:2905.
 151. Rajnicek A, McCaig C. Guidance of CNS growth cones by substratum grooves and

- ridges: effects of inhibitors of the cytoskeleton, calcium channels and signal transduction pathways. *J Cell Sci* 1997; 110 (Pt 23):2915–24.
152. Britland S, McCaig C. Embryonic *Xenopus* neurites integrate and respond to simultaneous electrical and adhesive guidance cues. *Exp Cell Res* 1996; 226(1):31–8.
 153. Buettner HM, Pittman RN. Quantitative effects of laminin concentration on neurite outgrowth in vitro. *Dev Biol* 1991; 145(2):266–76.
 154. Lemmon V, Burden SM, Payne HR, Elmslie GJ, Hlavin ML. Neurite growth on different substrates—permissive versus instructive influences and the role of adhesive strength. *J Neurosci* 1992; 12(3):818–26.
 155. Jimbo Y, Robinson HPC, Kawana A. Simultaneous measurement of intracellular calcium and electrical activity from patterned neural networks in culture. *IEEE Trans Biomed Eng* 1993; 40(8):804–810.
 156. Ravenscroft MS, Bateman KE, Shaffer KM, Schessler HM, Jung DR, Schneider TW, et al. Developmental neurobiology implications from fabrication and analysis of hippocampal neuronal networks on patterned silane-modified surfaces. *J Am Chem Soc* 1998; 120(47):12169.
 157. Ma W, Liu QY, Jung D, Manos P, Pancrazio JJ, Schaffner AE, et al. Central neuronal synapse formation on micropatterned surfaces. *Brain Res Dev Brain Res* 1998; 111(2): 231–43.
 158. Liu QY, Coulombe M, Dumm J, Shaffer KM, Schaffner AE, Barker JL, et al. Synaptic connectivity in hippocampal neuronal networks cultured on micropatterned surfaces. *Brain Res Dev Brain Res* 2000; 120(2):223–31.
 159. Fromherz P, Offenhausser A, Vetter T, Weis J. A neuron-silicon junction: a Retzius cell of the leech on an insulated-gate field-effect transistor. *Science* 1991; 252(5010):1290–3.
 160. Offenhausser A, Sprossler C, Matsuzawa M, Knoll W. Field-effect transistor array for monitoring electrical activity from mammalian neurons in culture. *Biosens Bioelectron* 1997; 12(8):819–26.
 161. Fromherz P, Stett A. Silicon-neuron junction—capacitive stimulation of an individual neuron on a silicon chip. *Phys Rev Lett* 1995; 75(8):1670–3.
 162. Litke A, Meister M. The retinal readout array. *Nucl Instrum Methods Phys Res Sect A Accel Spectrom Dect Assoc Equip* 1991; 310(1–2):389.
 163. Meister M, Pine J, Baylor DA. Multi-neuronal signals from the retina—acquisition and analysis. *J Neurosci Methods* 1994; 51(1):95.
 164. Thomas CA Jr, Springer PA, Loeb GE, Berwald-Netter Y, Okun LM. A miniature microelectrode array to monitor the bioelectric activity of cultured cells. *Exp Cell Res* 1972; 74:61.
 165. Gross GW, Wen WY, Lin JW. Transparent indium-tin oxide electrode patterns for extracellular, multisite recording in neuronal cultures. *J Neurosci Methods* 1985; 15(3): 243–52.
 166. Novak JL, Wheeler BC. Recording from the *Aplysia* abdominal ganglion with a planar microelectrode array. *IEEE Trans Biomed Eng* 1986; 33(2):196–202.
 167. Regehr WG, Pine J, Cohan CS, Mischke MD, Tank DW. Sealing cultured invertebrate neurons to embedded dish electrodes facilitates long-term stimulation and recording. *J Neurosci Methods* 1989; 30(2):91.
 168. Bove M, Grattarola M, Verreschi G. In vitro 2-D networks of neurons characterized by processing the signals recorded with a planar microtransducer array. *IEEE Trans Biomed Eng* 1997; 44(10):964–77.

169. Meister M, Berry MJ. The neural code of the retina. *Neuron* 1999; 22(3):435.
170. Berry MJ, Brivanlou IH, Jordan TA, Meister M. Anticipation of moving stimuli by the retina. *Nature* 1999; 398(6725):334.
171. Berry MJ, Meister M. Refractoriness and neural precision. *J Neurosci* 1998; 18(6): 2200.
172. Egert U, Schlosshauer B, Fennrich S, Nisch W, Fejtl M, Knott T, et al. A novel organotypic long-term culture of the rat hippocampus on substrate-integrated multielectrode arrays. *Brain Res Protoc* 1998; 2(4):229–42.
173. Jahnsen H, Kristensen BW, Thiebaud P, Noraberg J, Jakobsen B, Bove M, et al. Coupling of organotypic brain slice cultures to silicon-based arrays of electrodes. *Methods* 1999; 18(2):160.
174. Wilson RJ, Breckenridge L, Blackshaw SE, Connolly P, Dow JA, Curtis AS, et al. Simultaneous multisite recordings and stimulation of single isolated leech neurons using planar extracellular electrode arrays. *J Neurosci Methods* 1994; 53(1):101–10.
175. Breckenridge LJ, Wilson RJ, Connolly P, Curtis AS, Dow JA, Blackshaw SE, et al. Advantages of using microfabricated extracellular electrodes for in vitro neuronal recording. *J Neurosci Res* 1995; 42(2):266–76.
176. Shahaf G, Marom S. Learning in networks of cortical neurons. *J Neurosci* 2001; 21(22): 8782–8.
177. Ignatius MJ, Sawhney N, Gupta A, Thibadeau BM, Monteiro OR, Brown IG. Bioactive surface coatings for nanoscale instruments: effects on CNS neurons. *J Biomed Mater Res* 1998; 40(2):264–74.
178. James CD, Davis R, Meyer M, Turner A, Turner S, Withers G, et al. Aligned micro-contact printing of micrometer-scale poly-L-lysine structures for controlled growth of cultured neurons on planar microelectrode arrays. *IEEE Trans Biomed Eng* 2000; 47(1):17–21.
179. Griscom L, Degenaar P, LePioufle B, Tamiya E, Fujita H. Techniques for patterning and guidance of primary culture neurons on micro-electrode arrays. *Sens Actuator B Chem* 2002; 83(1–3):15–21.
180. Rutten W, Mouveroux JM, Buitenweg J, Heida C, Ruardij T, Marani E, et al. Neuroelectronic interfacing with cultured multielectrode arrays toward a cultured probe. *Proc IEEE* 2001; 89(7):1013–29.
181. Nisch W, Bock J, Egert U, Hammerle H, Mohr A. A thin film microelectrode array for monitoring extracellular neuronal activity in vitro. *Biosens Bioelectron* 1994; 9(9–10): 737–41.
182. Cui XY, Lee VA, Raphael Y, Wiler JA, Hetke JF, Anderson DJ, et al. Surface modification of neural recording electrodes with conducting polymer/biomolecule blends. *J Biomed Mater Res* 2001; 56(2):261–72.
183. Maher MP, Pine J, Wright J, Tai YC. The neurochip: a new multielectrode device for stimulating and recording from cultured neurons. *J Neurosci Methods* 1999; 87(1): 45.
184. Heida T, Rutten WL, Marani E. Dielectrophoretic trapping of dissociated fetal cortical rat neurons. *IEEE Trans Biomed Eng* 2001; 48(8):921–30.
185. Heida T, Vulto P, Rutten WL, Marani E. Viability of dielectrophoretically trapped neural cortical cells in culture. *J Neurosci Methods* 2001; 110(1–2):37–44.
186. Neher E. Ion Channels for communication between and within cells. *Science* 1992; 256(5056):498–502.

187. Schmidt C, Mayer M, Vogel H. A chip-based biosensor for the functional analysis of single ion channels. *Angew Chem Int Edit* 2000; 39(17):3137–40.
188. Pantoja R, Sigg D, Blunck R, Bezanilla F, Heath JR. Bilayer reconstitution of voltage-dependent ion channels using a microfabricated silicon chip. *Biophys J* 2001; 81(4):2389–94.
189. Klemic KG, Klemic JF, Reed MA, Sigworth FJ. Micromolded PDMS planar electrode allows patch clamp electrical recordings from cells. *Biosens Bioelectron* 2002; 17(6–7):597–604.
190. Lehnert T, Gijs MAM, Netzer R, Bischoff U. Realization of hollow SiO₂ micronozzles for electrical measurements on living cells. *Appl Phys Lett* 2002; 81(26):5063–5.
191. Fertig N, Blick RH, Behrends JC. Whole cell patch clamp recording performed on a planar glass chip. *Biophys J* 2002; 82(6):3056–62.
192. Fertig N, Meyer C, Blick RH, Trautmann C, Behrends JC. Microstructured glass chip for ion-channel electrophysiology. *Phys Rev E* 2001; 6404(4):#040901.
193. Fertig N, Tilke A, Blick RH, Kotthaus JP, Behrends JC, ten Bruggencate G. Stable integration of isolated cell membrane patches in a nanomachined aperture. *Appl Phys Lett* 2000; 77(8):1218–20.
194. Fertig N, Klau M, George M, Blick RH, Behrends JC. Activity of single ion channel proteins detected with a planar microstructure. *Appl Phys Lett* 2002; 81(25):4865–7.
195. Taylor AM, Rhee SW, Tu CH, Cribbs DH, Cotman CW, Jeon NL. Microfluidic multicompartiment device for neuroscience research. *Langmuir* 2003; 19(5):1551–6.
196. Pancrazio JJ, Whelan JP, Borkholder DA, Ma W, Stenger DA. Development and application of cell-based biosensors. *Ann Biomed Eng* 1999; 27(6):697–711.
197. Stenger DA, Gross GW, Keefer EW, Shaffer KM, Andreadis JD, Ma W, et al. Detection of physiologically active compounds using cell-based biosensors. *Trends Biotechnol* 2001; 19(8):304–9.
198. Gross GW, Rhoades BK, Azzazy HM, Wu MC. The use of neuronal networks on multielectrode arrays as biosensors. *Biosens Bioelectron* 1995; 10(6–7):553–67.
199. Morefield SI, Keefer EW, Chapman KD, Gross GW. Drug evaluations using neuronal networks cultured on microelectrode arrays. *Biosens Bioelectron* 2000; 15(7–8):383–96.
200. Keefer EW, Norton SJ, Boyle NA, Talesa V, Gross GW. Acute toxicity screening of novel AChE inhibitors using neuronal networks on microelectrode arrays. *Neurotoxicology* 2001; 22(1):3–12.
201. Bove M, Martinoia S, Verreschi G, Giugliano M, Grattarola M. Analysis of the signals generated by networks of neurons coupled to planar arrays of microtransducers in simulated experiments. *Biosens Bioelectron* 1998; 13(6):601.
202. Chiappalone M, Vato A, Tedesco M, Marcoli M, Davide F, Martinoia S. Networks of neurons coupled to microelectrode arrays: a neuronal sensory system for pharmacological applications. *Biosens Bioelectron* 2003; 18(5–6):627–34.
203. DeBusschere BD, Kovacs GT. Portable cell-based biosensor system using integrated CMOS cell-cartridges. *Biosens Bioelectron* 2001; 16(7–8):543–56.
204. Westermark B. Growth control in miniclones of human glial cells. *Exp Cell Res* 1978; 111:295–9.
205. St. John PM, Kam L, Turner SW, Craighead HG, Issacson M, Turner JN, et al. Preferential glial cell attachment to microcontact printed surfaces. *J Neurosci Meth* 1997; 75(2):171.

206. Kam L, Shain W, Turner JN, Bizios R. Correlation of astroglial cell function on micro-patterned surfaces with specific geometric parameters. *Biomaterials* 1999; 20(23–24): 2343–50.
207. Kam L, Shain W, Turner JN, Bizios R. Selective adhesion of astrocytes to surfaces modified with immobilized peptides. *Biomaterials* 2002; 23(2):511–5.
208. Turner S, Kam L, Isaacson M, Craighead HG, Shain W, Turner J. Cell attachment on silicon nanostructures. *J Vac Sci Technol B* 1997; 15(6):2848.
209. Craighead HG, James CD, Turner AMP. Chemical and topographical patterning for directed cell attachment. *Curr Opin Solid State Mater Sci* 2001; 5(2–3):177–84.
210. Craighead HG, Turner SW, Davis RC, Perez AM, St. John PM, Isaacson MS, et al. Chemical and topographical surface modification for control of central nervous system cell adhesion. *J Biomed Microdev* 1998; 1(1):49–64.
211. Takano H, Sul JY, Mazzanti ML, Doyle RT, Haydon PG, Porter MD. Micropatterned substrates: approach to probing intercellular communication pathways. *Anal Chem* 2002; 74(18):4640–6.
212. Webb A, Clark P, Skepper J, Compston A, Wood A. Guidance of oligodendrocytes and their progenitors by substratum topography. *J Cell Sci* 1995; 108(Pt 8):2747–60.
213. Detrait E, Lhoest JB, Bertrand P, van den Bosch de Aguilar P. Fibronectin-pluronic coadsorption on a polystyrene surface with increasing hydrophobicity: relationship to cell adhesion. *J Biomed Mater Res* 1999; 45(4):404–13.
214. Thompson DM, Buettner HM. Schwann cell response to micropatterned laminin surfaces. *Tiss Eng* 2001; 7(3):247–65.
215. Turner DC, Lawton J, Dollenmeier P, Ehrismann R, Chiquet M. Guidance of myogenic cell migration by oriented deposits of fibronectin. *Dev Biol* 1983; 95:497–504.
216. Clark P, Coles D, Peckham M. Preferential adhesion to and survival on patterned laminin organizes myogenesis in vitro. *Exp Cell Res* 1997; 230(2):275–83.
217. Lieberman M, Roggeveen AE, Purdy JE, Johnson EA. Synthetic strands of cardiac muscle: growth and physiological implication. *Science* 1972; 175:909–11.
218. Lieberman M, Sawanabori T, Kootsey JM, Johnson EA. A synthetic strand of cardiac muscle: its passive electrical properties. *J Gen Physiol* 1975; 65:527–50.
219. Horres CR, Lieberman M, Purdy JE. Growth orientation of heart cells on nylon monofilament. *J Membr Biol* 1977; 34:313–29.
220. Rohr S, Scholly DM, Kleber AG. Patterned growth of neonatal rat heart cells in culture. Morphological and electrophysiological characterization. *Circ Res* 1991; 68(1): 114–30.
221. Rohr S, Salzberg BM. Multiple site optical recording of transmembrane voltage (MSORTV) in patterned growth heart cell cultures: assessing electrical behavior, with microsecond resolution, on a cellular and subcellular scale. *Biophys J* 1994; 67(3):1301–15.
222. Rohr S. Determination of impulse conduction characteristics at a microscopic scale in patterned growth heart cell cultures using multiple site optical recording of transmembrane voltage. *J Cardiovasc Electrophysiol* 1995; 6(7):551–68.
223. Thomas SP, Bircher-Lehmann L, Thomas SA, Zhuang J, Saffitz JE, Kleber AG. Synthetic strands of neonatal mouse cardiac myocytes: structural and electrophysiological properties. *Circ Res* 2000; 87(6):467–73.
224. Thomas SP, Kucera JP, Bircher-Lehmann L, Rudy Y, Saffitz JE, Kleber AG. Impulse propagation in synthetic strands of neonatal cardiac myocytes with genetically reduced levels of connexin43. *Circ Res* 2003; 92(11):1209–16.

225. McDevitt TC, Angello JC, Whitney ML, Reinecke H, Hauschka SD, Murry CE, et al. In vitro generation of differentiated cardiac myofibers on micropatterned laminin surfaces. *J Biomed Mater Res* 2002; 60(3):472–9.
226. Kaji H, Takoh K, Nishizawa M, Matsue T. Intracellular Ca^{2+} imaging for micropatterned cardiac myocytes. *Biotechnol Bioeng* 2003; 81(6):748–51.
227. Gopalan SM, Flaim C, Bhatia SN, Hoshijima M, Knoell R, Chien KR, et al. Anisotropic stretch-induced hypertrophy in neonatal ventricular myocytes micropatterned on deformable elastomers. *Biotechnol Bioeng* 2003; 81(5):578–87.
228. Deutsch J, Motiagh D, Russell B, Desai TA. Fabrication of microtextured membranes for cardiac myocyte attachment and orientation. *J Biomed Mater Res* 2000; 53(3):267–75.
229. Motlagh D, Senyo SE, Desai TA, Russell B. Microtextured substrata alter gene expression, protein localization and the shape of cardiac myocytes. *Biomaterials* 2003; 24(14):2463–76.
230. Connolly P, Clark P, Curtis AS, Dow JA, Wilkinson CD. An extracellular microelectrode array for monitoring electrogenic cells in culture. *Biosens Bioelectron* 1990; 5(3):223–34.
231. Denyer MCT, Riehle M, Britland ST, Offenhauser A. Preliminary study on the suitability of a pharmacological bio-assay based on cardiac myocytes cultured over microfabricated microelectrode arrays. *Med Biol Eng Comput* 1998; 36(5):638–44.
232. Aravanis AM, DeBusschere BD, Chruscinski AJ, Gilchrist KH, Kobilka BK, Kovacs GT. A genetically engineered cell-based biosensor for functional classification of agents. *Biosens Bioelectron* 2001; 16(7–8):571–7.
233. Soejima K, Negishi N, Nozaki M, Sasaki K. Effect of cultured endothelial cells on angiogenesis in vivo. *Plast Reconstr Surg* 1998; 101(6):1552–60.
234. Folkman J, Moscona A. Role of cell shape in growth control. *Nature* 1978; 273(5661):345–9.
235. Kapur R, Rudolph AS. Cellular and cytoskeleton morphology and strength of adhesion of cells on self-assembled monolayers of organosilanes. *Exp Cell Res* 1998; 244(1):275.
236. Matsuda T, Inoue K, Sugawara T. Development of micropatterning technology for cultured cells. *Am Soc Artif Intern Organ Trans* 1990; 36(3):M559–62.
237. Matsuda T, Sugawara T. Development of surface photochemical modification method for micropatterning of cultured cells. *J Biomed Mater Res* 1995; 29(6):749–56.
238. Sugawara T, Matsuda T. Photochemical surface derivatization of a peptide containing Arg-Gly-Asp (RGD). *J Biomed Mater Res* 1995; 29(9):1047–52.
239. Spargo BJ, Testoff MA, Nielsen TB, Stenger DA, Hickman JJ, Rudolph AS. Spatially controlled adhesion, spreading, and differentiation of endothelial cells on self-assembled molecular monolayers. *Proc Natl Acad Sci USA* 1994; 91(23):11070–4.
240. Mrksich M, Dike LE, Tien J, Ingber DE, Whitesides GM. Using microcontact printing to pattern the attachment of mammalian cells to self-assembled monolayers of alkanethiolates on transparent films of gold and silver. *Exp Cell Res* 1997; 235(2):305–13.
241. Roberts C, Chen CS, Mrksich M, Martichonok V, Ingber DE, Whitesides GM. Using mixed self-assembled monolayers presenting RGD and (EG)(3)OH groups to characterize long-term attachment of bovine capillary endothelial cells to surfaces. *J Am Chem Soc* 1998; 120(26):6548.

242. Tidwell CD, Ertel SI, Ratner BD, Tarasevich BJ, Atre S, Allara DL. Endothelial cell growth and protein adsorption on terminally functionalized, self-assembled monolayers of alkanethiolates on gold. *Langmuir* 1997; 13(13):3404.
243. Ostuni E, Chapman RG, Liang MN, Meluleni G, Pier G, Ingber DE, et al. Self-assembled monolayers that resist the adsorption of proteins and the adhesion of bacterial and mammalian cells. *Langmuir* 2001; 17(20):6336–43.
244. Chen CS, Mrksich M, Huang S, Whitesides GM, Ingber DE. Geometric control of cell life and death. *Science* 1997; 276(5317):1425–8.
245. Huang S, Chen CS, Ingber DE. Control of cyclin D1, p27(Kip1), and cell cycle progression in human capillary endothelial cells by cell shape and cytoskeletal tension. *Mol Biol Cell* 1998; 9(11):3179.
246. Nelson CM, Chen CS. Cell-cell signaling by direct contact increases cell proliferation via a PI3K-dependent signal. *FEBS Lett* 2002; 514(2–3):238–42.
247. Matsuda T, Chung DJ. Microfabricated surface designs for cell culture and diagnosis. *Asaio J* 1994; 40(3):M594–7.
248. Dike LE, Chen CS, Mrksich M, Tien J, Whitesides GM, Ingber DE. Geometric control of switching between growth, apoptosis, and differentiation during angiogenesis using micropatterned substrates. *In Vitro Cell Dev Biol Anim* 1999; 35(8):441.
249. Parker KK, Brock AL, Brangwynne C, Mannix RJ, Wang N, Ostuni E, et al. Directional control of lamellipodia extension by constraining cell shape and orienting cell tractional forces. *FASEB J* 2002; 16(10):1195–204.
250. Li S, Bhatia S, Hu YL, Shin YT, Li YS, Usami S, et al. Effects of morphological patterning on endothelial cell migration. *Biorheology* 2001; 38(2–3):101–8.
251. Lee JW, Morgan JR, Tompkins RG, Yarmush ML. The importance of proline on long-term hepatocyte function in a collagen gel sandwich configuration—regulation of protein secretion. *Biotechnol Bioeng* 1992; 40(2):298.
252. Lee J, Morgan JR, Tompkins RG, Yarmush ML. Proline-mediated enhancement of hepatocyte function in a collagen gel sandwich culture configuration. *Faseb J* 1993; 7(6):586.
253. Dunn JCY, Tompkins RG, Yarmush ML. Hepatocytes in collagen sandwich—evidence for transcriptional and translational regulation. *J Cell Biol* 1992; 116(4):1043.
254. Ezzell RM, Toner M, Hendricks K, Dunn JCY, Tompkins RG, Yarmush ML. Effect of collagen gel configuration on the cytoskeleton in cultured rat hepatocytes. *Exp Cell Res* 1993; 208(2):442.
255. Moghe PV, Parashurama N, Ezzell RM, Toner M, Tompkins RG, Yarmush ML. Effect of collagen gel configuration on integrin localization in cultured rat hepatocytes. *Mol Biol Cell* 1995; 6:1648.
256. Moghe PV, Berthiaume F, Ezzell RM, Toner M, Tompkins RG, Yarmush ML. Culture matrix configuration and composition in the maintenance of hepatocyte polarity and function. *Biomaterials* 1996; 17(3):373.
257. Moghe PV, Cogger RN, Toner M, Yarmush ML. Cell-cell interactions are essential for maintenance of hepatocyte function in collagen gel but not on Matrigel. *Biotechnol Bioeng* 1997; 56(6):706.
258. Moghe PV, Ezzell RM, Toner M, Tompkins RG, Yarmush ML. Role of beta 1 integrin distribution in morphology and function of collagen-sandwiched hepatocytes. *Tissue Eng* 1997; 3(1):1.
259. Berthiaume F, Moghe PV, Toner M, Yarmush ML. Effect of extracellular matrix

- topology on cell structure, function, and physiological responsiveness: hepatocytes cultured in a sandwich configuration. *FASEB J* 1996; 10(13):1471.
260. Miyamoto S, Ohashi A, Kimura J, Tobe S, Akaike T. A novel approach for toxicity sensing using hepatocytes on a collagen-patterned plate. *Sens Actuator B Chem* 1993; 13(1–3):196.
 261. Dewez JL, Lhoest JB, Detrait E, Berger V, Dupont-Gillain CC, Vincent LM, et al. Adhesion of mammalian cells to polymer surfaces: from physical chemistry of surfaces to selective adhesion on defined patterns. *Biomaterials* 1998; 19(16):1441.
 262. Singhvi R, Kumar A, Lopez GP, Stephanopoulos GN, Wang DI, Whitesides GM, et al. Engineering cell shape and function. *Science* 1994; 264(5159):696–8.
 263. Takezawa T, Yamazaki M, Mori Y, Yonaha T, Yoshizato K. Morphological and immuno-cytochemical characterization of a hetero-spheroid composed of fibroblasts and hepatocytes. *J Cell Sci* 1992; 101:495.
 264. Yamato M, Konno C, Utsumi M, Kikuchi A, Okano T. Thermally responsive polymer-grafted surfaces facilitate patterned cell seeding and co-culture. *Biomaterials* 2002; 23(2):561–7.
 265. Bhatia SN, Balis UJ, Yarmush ML, Toner M. Probing heterotypic cell interactions: hepatocyte function in microfabricated co-cultures. *J Biomater Sci Polym Ed* 1998; 9(11):1137–60.
 266. Chehroudi B, Ratkay J, Brunette DM. The role of implant surface geometry on mineralization in vivo and in vitro—a transmission and scanning electron-microscopic study. *Cell Mater* 1992; 2(2):89.
 267. Qu J, Chehroudi B, Brunette DM. The use of micromachined surfaces to investigate the cell behavioural factors essential to osseointegration. *Oral Dis* 1996; 2(1):102–15.
 268. Chehroudi B, McDonnell D, Brunette DM. The effects of micromachined surfaces on formation of bonelike tissue on subcutaneous implants as assessed by radiography and computer image processing. *J Biomed Mater Res* 1997; 34(3):279–90.
 269. Healy KE, Lom B, Hockberger PE. Spatial distribution of mammalian cells dictated by material surface chemistry. *Biotechnol Bioeng* 1994; 43(8):792.
 270. Thomas CH, McFarland CD, Jenkins ML, Rezanian A, Steele JG, Healy KE. The role of vitronectin in the attachment and spatial distribution of bone-derived cells on materials with patterned surface chemistry. *J Biomed Mater Res* 1997; 37(1):81.
 271. Rezanian A, Thomas CH, Healy KE. A probabilistic approach to measure the strength of bone cell adhesion to chemically modified surfaces. *Ann Biomed Eng* 1997; 25(1):190–203.
 272. Healy KE, Thomas CH, Rezanian A, Kim JE, McKeown PJ, Lom B, et al. Kinetics of bone cell organization and mineralization on materials with patterned surface chemistry. *Biomaterials* 1996; 17(2):195–208.
 273. Rezanian A, Thomas CH, Branger AB, Waters CM, Healy KE. The detachment strength and morphology of bone cells contacting materials modified with a peptide sequence found within bone sialoprotein. *J Biomed Mater Res* 1997; 37(1):9.
 274. Rezanian A, Healy KE. Biomimetic peptide surfaces that regulate adhesion, spreading, cytoskeletal organization, and mineralization of the matrix deposited by osteoblast-like cells. *Biotechnol Progr* 1999; 15(1):19.
 275. Hasenbein ME, Andersen TT, Bizios R. Micropatterned surfaces modified with select peptides promote exclusive interactions with osteoblasts. *Biomaterials* 2002; 23(19):3937–42.

276. Bearinger JP, Castner DG, Golledge SL, Rezania A, Hubchak S, Healy KE. P(AAm-co-EG) interpenetrating polymer networks grafted to oxide surfaces: surface characterization, protein adsorption, and cell detachment studies. *Langmuir* 1997; 13(19): 5175.
277. Thomas CH, Lhoest JB, Castner DG, McFarland CD, Healy KE. Surfaces designed to control the projected area and shape of individual cells. *J Biomech Eng* 1999; 121(1): 40.
278. Bearinger JP, Castner DG, Healy KE. Biomolecular modification of p(AAm-co-EG/AA) IPNs supports osteoblast adhesion and phenotypic expression. *J Biomater Sci Polym Ed* 1998; 9(7):629–52.
279. Barber TA, Golledge SL, Castner DG, Healy KE. Peptide-modified p(AAm-co-EG/AAc) IPNs grafted to bulk titanium modulate osteoblast behavior in vitro. *J Biomed Mater Res* 2003; 64(1):38–47.
280. Stile RA, Healy KE. Thermo-responsive peptide-modified hydrogels for tissue regeneration. *Biomacromolecules* 2001; 2(1):185–94.
281. Stile RA, Healy KE. Poly(*N*-isopropylacrylamide)-based semi-interpenetrating polymer networks for tissue engineering applications. 1. Effects of linear poly(acrylic acid) chains on phase behavior. *Biomacromolecules* 2002; 3(3):591–600.
282. Ogura E, Abatti PJ, Moriizumi T. Measurement of human red blood cell deformability using a single micropore on a thin Si₃N₄ film. *IEEE Trans Biomed Eng* 1991; 38(8): 721–6.
283. Brody J, Austin B, Bitensky M. Red-blood-cell flow-through a microfabricated structure. *Biophys J* 1994; 66(2):A85.
284. Brody J, Han Y, Austin R, Bitensky M. Deformation and flow of red blood cells in a synthetic lattice: evidence for an active cytoskeleton. *Biophys J* 1995; 68(6): 2224–32.
285. Shevkoplyas SS, Gifford SC, Yoshida T, Bitensky MW. Prototype of an in vitro model of the microcirculation. *Microvasc Res* 2003; 65(2):132–6.
286. Gifford SC, Frank MG, Derganc J, Gabel C, Austin RH, Yoshida T, et al. Parallel microchannel-based measurements of individual erythrocyte areas and volumes. *Biophys J* 2003; 84(1):623–33.
287. Shelby JP, Lim DS, Kuo JS, Chiu DT. Microfluidic systems: high radial acceleration in microvortices. *Nature* 2003; 425(6953):38.
288. Tan J, Shen H, Carter KL, Saltzman WM. Controlling human polymorphonuclear leukocytes motility using microfabrication technology. *J Biomed Mater Res* 2000; 51(4):694–702.
289. Tan J, Shen H, Saltzman WM. Micron-scale positioning of features influences the rate of polymorphonuclear leukocyte migration. *Biophys J* 2001; 81(5):2569–79.
290. Jeon NL, Baskaran H, Dertinger SKW, Whitesides GM, Van de Water L, Toner M. Neutrophil chemotaxis in linear and complex gradients of interleukin-8 formed in a microfabricated device. *Nat Biotechnol* 2002; 20(8):826–30.
291. Hoch HC, Staples RC, Whitehead B, Comeau J, Wolf ED. Signaling for growth orientation and cell differentiation by surface topography in *Uromyces*. *Science* 1987; 235:1659–62.
292. Glasgow IK, Zeringue HC, Beebe DJ, Choi SJ, Lyman JT, Chan NG, et al. Handling individual mammalian embryos using microfluidics. *IEEE Trans Biomed Eng* 2001; 48(5):570–8.

293. Wheeler MB, Clark SG, Beebe DJ. Developments in in vitro technologies for swine embryo production. *Reprod Fertil Dev* 2004; 16(2):15–25.
294. Suh RS, Phadke N, Ohl DA, Takayama S, Smith GD. In vitro fertilization within microfluidic channels requires lower total numbers and lower concentrations of spermatozoa. *Fertil Steril* 2003; 80(O109, Suppl. 3):S42.
295. Mao H, Cremer PS, Manson MD. A sensitive, versatile microfluidic assay for bacterial chemotaxis. *Proc Natl Acad Sci USA* 2003; 100(9):5449–54.